(NASA-CR-158479) IMPROVED HIGH MODULUS CARBON FIBERS (Rensselaer Polytechnic Inst., Troy, N. Y.) 81 p HC A05/MF A01 CSCL 11D

N79-21134

Unclas

G3/24 23972

"IMPROVED HIGH MODULUS CARBON FIBERS"

NASA GRANT NO. NSG 1510

G. S. ANSELL

S. H. CHEN

R. J. DIEFENDORF

C. M. KIM

C. W. LEMAISTRE

C. E. LYMAN

T. H. SHEN

J. J-H. WANG

RENSSELAER POLYTECHNIC INSTITUTE

TROY, NEW YORK 12181

APRIL 1979

FOREWORD

This report was prepared at Rensselaer Polytechnic Institute, Troy, New York, under NASA Grant No. NSG1510. The report covers the research completed in the first year of the program, April 1, 1978 through March 31, 1979. The program is sponsored by the National Aeronautics and Space Administration (NASA), Langley Research Center. The principal Investigator for Rensselaer Polytechnic Institute is Dr. G. S. Ansell. Dr. R. T. Swann is project manager for NASA, Langley.

TABLE OF CONTENTS

LIST OF FIGURES

LIST OF FIGURES (cont'd.)

LIST OF TABLES

I. INTRODUCTION

Carbon fiber reinforced plastics will find greater usage due to an increasing demand for high modulus, low weight materials. Carbon fibers have low specific density, high modulus, high strength, and also high electrical conductivity. Being an electrical conductor carbon fibers may create an electrical hazard if these fibers are released into the environment. The electrical problem is compounded because of the size, density, and chemical inertness of carbon fibers. Due to the lightness and the micron size diameter, one carbon fiber behaves like an aerosol. Once released into the atmosphere carbon fibers float and drift with air currents. This implies that an accidental release of carbon fibers may contaminate a large area downwind from the origin of the accident. In fact, electrical problems created by carbon fibers may be everlasting since carbon fibers are chemically inert and will not degrade with time.

The goal of this research is to develop new carbon fibers which are electrical insulating and still maintain the mechanical properties of the original carbon fibers. Three approaches were taken to increase the electrical resistance of carbon fibers

(1) Boron nitride (BN) coatings,

(2) Doping of carbon fibers to alter their electrical properties,

(3) Low temperature final heat treatment.

Boron nitride coating of carbon fiber produces a highly insulating fiber with just small reductions in both strength and modulus. It is found that a thin coating (.5 micron) increases the electrical resistance of carbon fibers from (2000 ohms/cm of fiber) to greater than (10^9 ohms/cm of fiber). The breakdown voltage of the insulating BN coating is greater than 350 volts.

Preliminary attempts to dope carbon fibers have failed to alter the electrical properties of the fibers. Both nitrogen and boron dopants were found to have small effects.

The third approach which relies on low temperature heat treatment is actively being pursued. Studies are being run to try to achieve higher preferred orientations (successfully) in the precursor, and to minimize the loss of this preferred orientation in subsequent processing. The experiments are underway and preliminary results should be completed during the next six months.

Additional work was performed to better understand the structure of carbon fibers and its effect upon properties. This work includes:

(1) Determination of electrical conductivity within carbon fibers,

(2) Determination of preferred orientation at the interior of a fiber,

(3) Measurement of axial residual stresses within a carbon fiber.

Boron Nitride

Boron nitride is the best insulator known. The resistivity of boron nitride (graphite structure allotrope) is too high to measure at room temperature. The conductivity of BN, however, can be measured at high temperatures and with an extrapolation of data (Fig. 1) to room temperature, can be estimated as conductivity of BN is less than 10^{-16} $(\Omega\text{-cm})^{-1}$. Aside from its good insulating property, and voltage breakdown strength, BN was chosen as it has a planar structure similar to that of graphite and the structure at the surface of PAN based carbon fibers. The similarity of the coefficient of thermal expansion and modulus for the two materials (BN and C) offers a better chance for a compatible coating of BN on carbon fibers to be achieved.

II. EXPERIMENTAL

(1) BN Coating

A resistance heated graphite furnace was used to vapor deposit a boron nitride on carbon fibers (Fig. 2). PAN fibers (Fortafil 4R and Hercules AS-1), in yarn form, were used to substrate. Experiments were carried out below 1450°C since such temperatures will not drastically alter the properties of the carbon fibers. Table I shows the treatment

(2) Structure Determination

X-ray diffraction, TEM, SEM, and optical microscopy were used to determine the structure of the coated carbon fibers

FIGURE 1

CONDUCTIVITY OF BORON NITRIDE WITH CONCENTRATION OF CARBON.

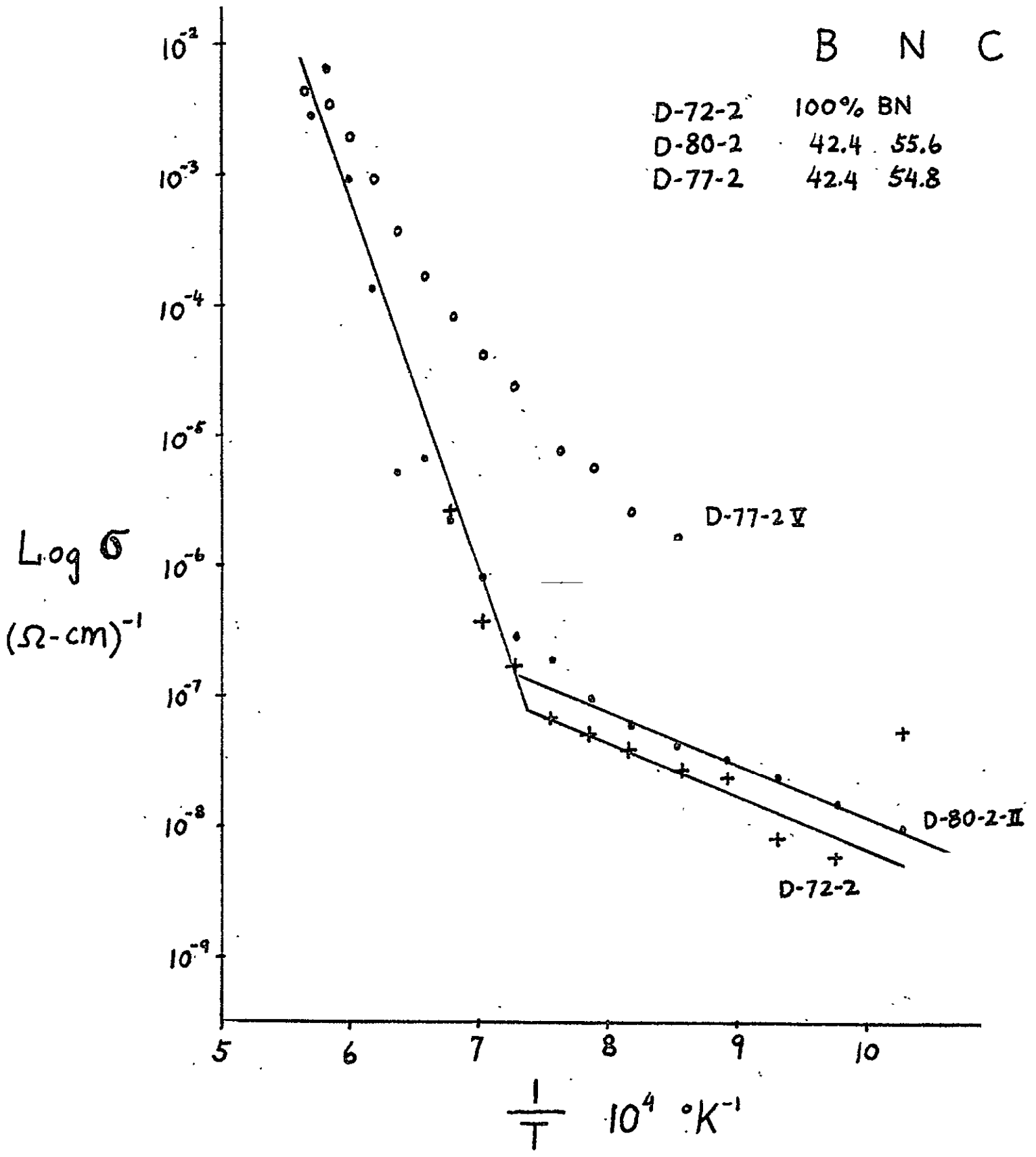
B N C
D-72-2 100% BN
D-80-2 42.4 55.6
D-77-2 42.4 54.8
D-77-2 V
D-80-2-II
D-72-2
Log σ
(Ω-cm)⁻¹
10⁻²
10⁻³
10⁻⁴
10⁻⁵
10⁻⁶
10⁻⁷
10⁻⁸
10⁻⁹
5
6
7
8
9
10
1/T 10⁴ °K⁻¹

FIGURE 2

COATING APPARATUS

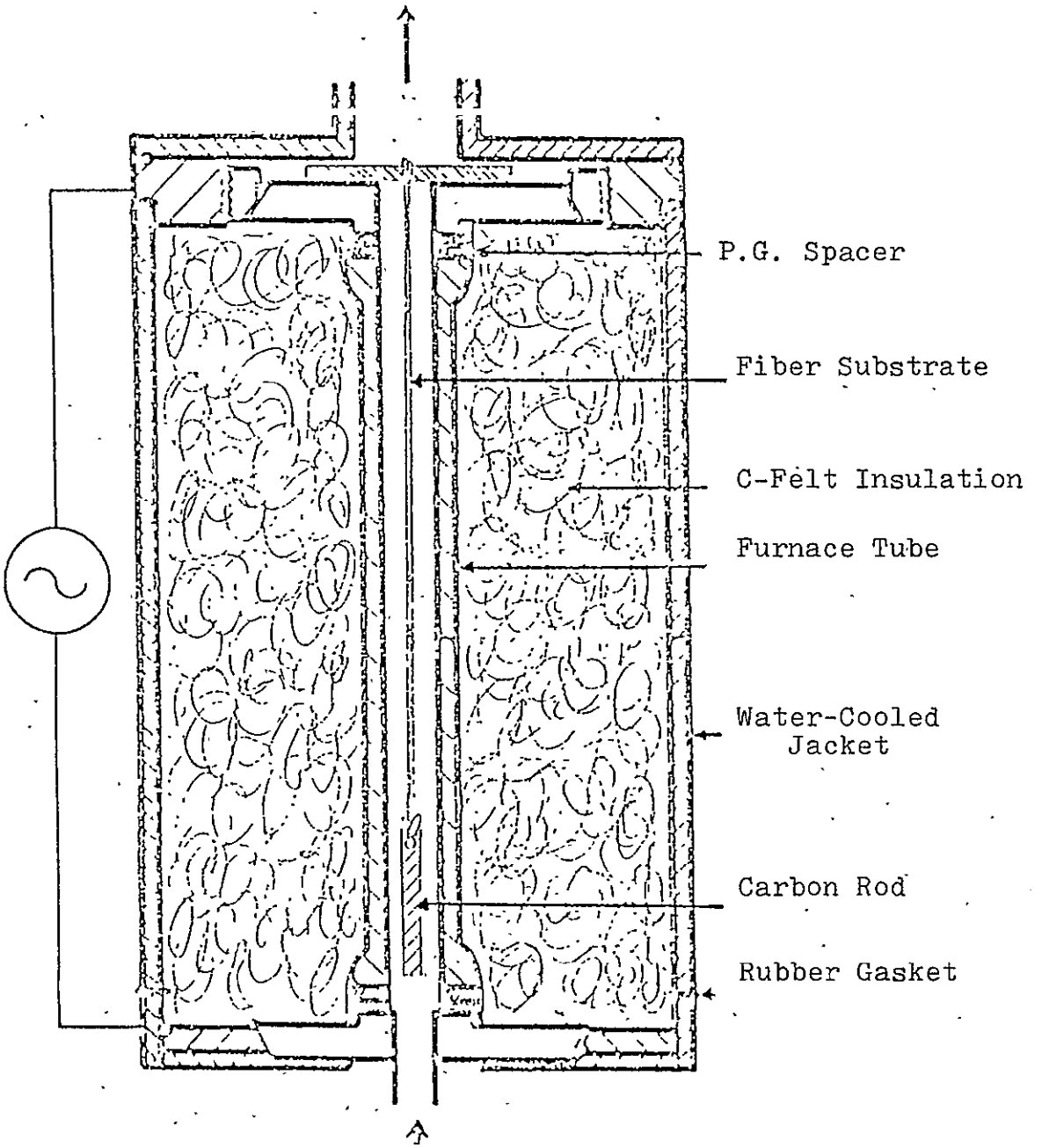

TABLE I

BN COATING

Temp. (°C)	Time (Second)	Pressure (Torr)	Flow Rate (cfh) BCl_3	NH_3	
885	30	1.16	0.75	0.50	
1000	30	0.85	0.75	0.50	
1150	30	0.82	0.75	0.50	
1150	30	0.82	0.75	0.50	BCl_3 1st
1150	30	0.40	0.50	0.50	
1150	30	0.46	0.50	0.75	
1150	30	0.45	0.38	0.28	
1150	30	0.53	0.25	0.75	
1150	30	1.00	0.75	0.25	
1150	30	0.82	0.75	0.50	Hercules (AS-1)
1150	15	0.84	0.75	0.50	
1150	60	1.10	0.75	0.50	
1290	30	0.86	0.75	0.50	
1430	30	1.15	0.75	0.50	

All samples were Fortafil 4R except Hercules sample mentioned.

All the samples were treated in the following order: NH_3 gas turned on, BCl_3 on, BCl_3 off and NH_3 off. Time was measured at the intervals between BCl_3 on and off. However, the sample which is mentioned as BCl_3 1st is BCl_3 gas turned on, NH_3 on, NH_3 off and BCl_3 off.

Figure 3 shows the schematic arrangements of a sample being observed with TEM. Samples were broken into small fragments and laid down on a copper double grid. The electron diffraction patterns of protruding surface layers revealed the identity of the coating.

(3) Electrical Properties Measurements

(A) Resistivity Measurement

The experimental arrangements are schematized in Fig. 4. A cross section of the fiber coating and measurement electrodes at line A-A is enlarged and displayed directly below the schematic of the apparatus (Fig. 4b). To insure conduction of an electrode with the conducting carbon fiber at the interior, silver paint was applied to one end of a BN coated carbon fiber (Electrode A). At Electrode B silver paint was applied around the surface of the fiber coating. The length between electrodes was 2 cm. It was assumed that there is negligible resistance to the path of current along the center of the carbon fiber between A and B. Ten volts of DC power was applied to the sample. The internal resistance of the voltmeter was about 10^7 ohms.

(B) Breakdown Voltage Measurement

Figure 5 shows schematic arrangements for the measurement of breakdown voltage. The distance between copper electrodes was 3 mm. The diameter of copper wire was 0.025 mm (#30). Figure 4b shows the arrangement of the electrodes touching the sample. A weight (56 g) was applied on the fiber

FIGURE 3

THE SCHEMATIC ARRANGEMENTS OF
THE SAMPLE IN TEM.

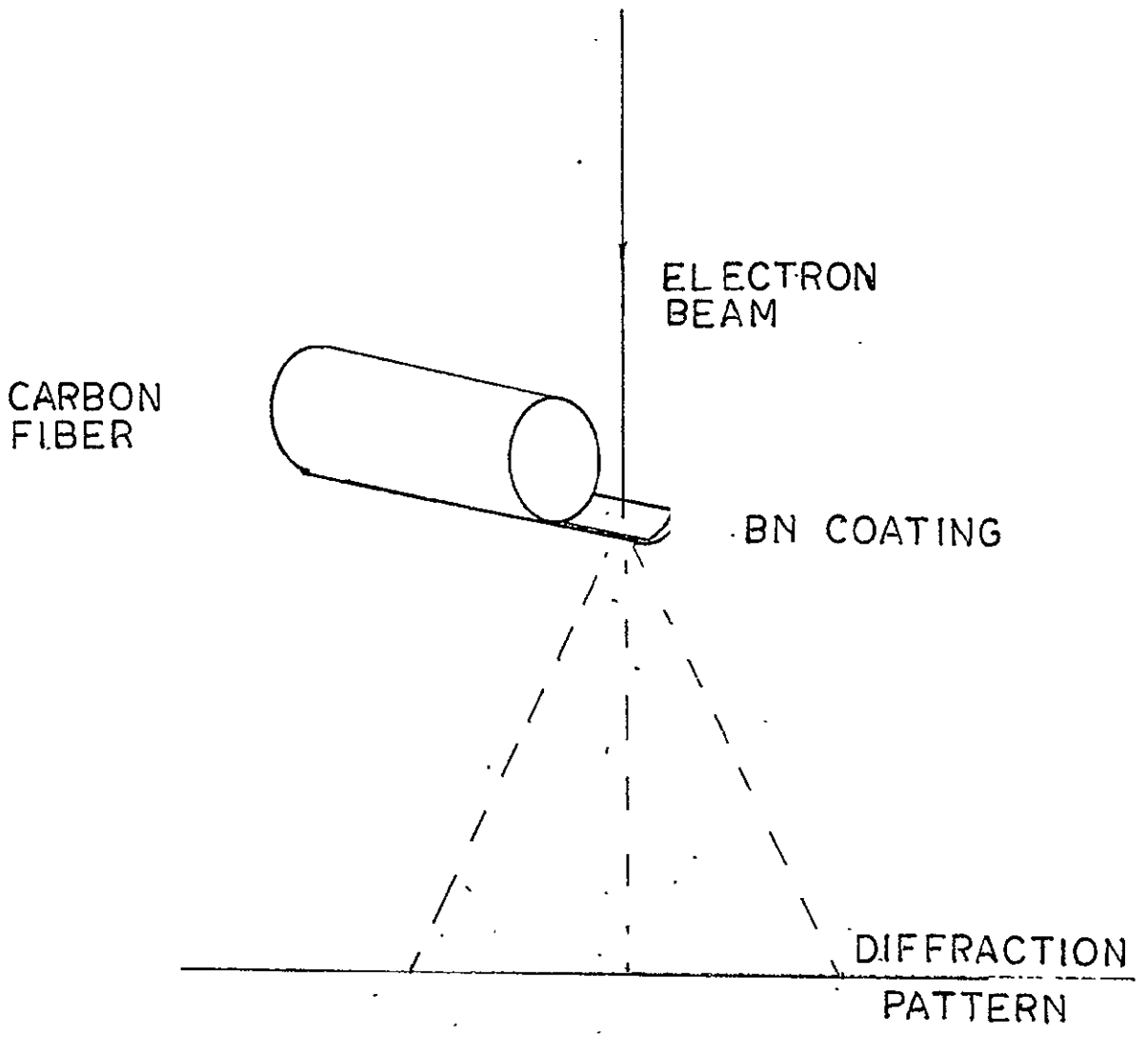
ELECTRON
BEAM
CARBON
FIBER
BN COATING
DIFFRACTION
PATTERN

FIGURE 4

SCHEMATIC DIAGRAM OF RESISTIVITY MEASUREMENT.

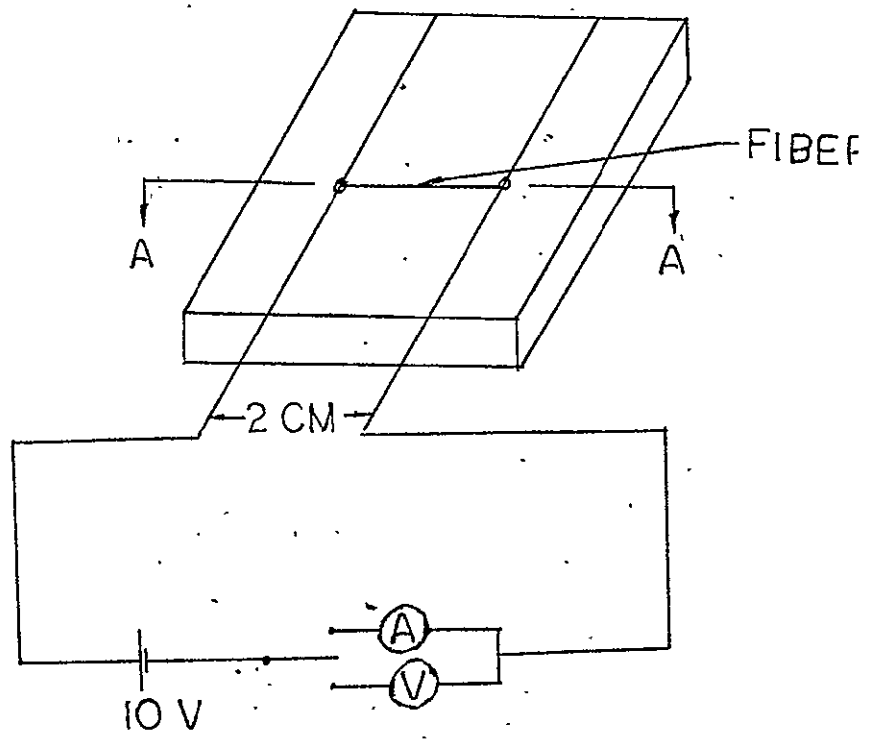
FIBER
A
A
2 CM
A
V
10 V

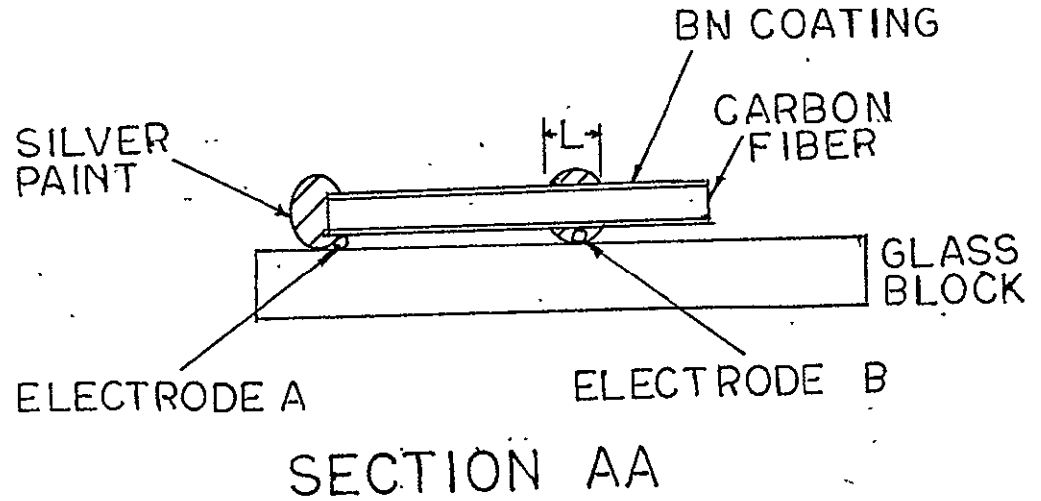
BN COATING
CARBON FIBER
L
SILVER PAINT
GLASS BLOCK
ELECTRODE A
ELECTRODE B

SECTION AA

FIGURE 5

SCHEMATIC DIAGRAM OF BREAKDOWN-MEASUREMENT.

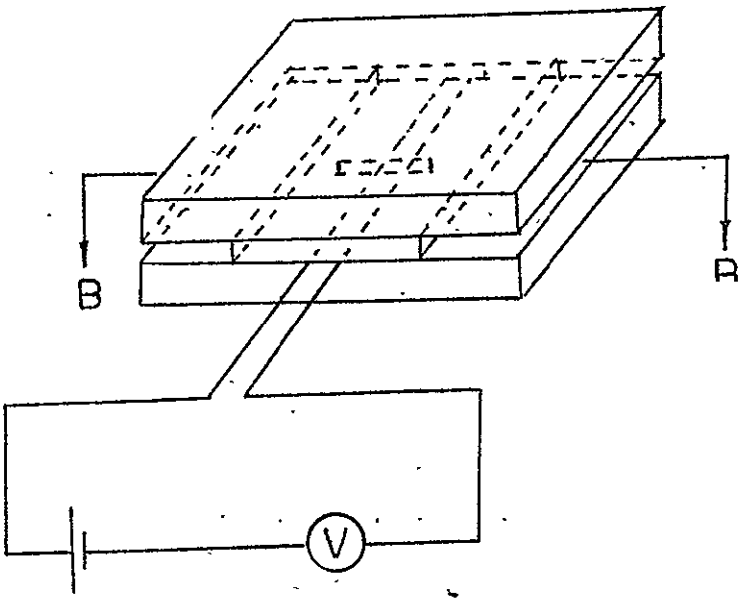

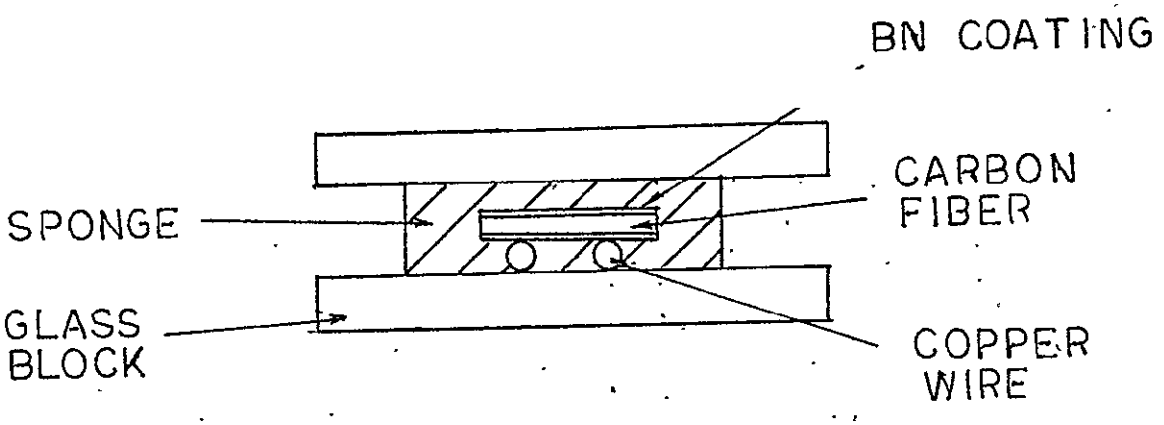

SECTION BB

to reduce the contact resistance. A 2 mm thick sponge was inserted between the fiber and weight to reduce damage to the coating during loading. A voltage drop is then developed between the electrodes through the BN coating. The voltage is gradually increased at constant rate. There are two sources of high resistance in this loop. One is the internal resistance of the voltmeter, about 10^{-7} ohm, and the other is the resistance of the coating which is much higher than that of the voltmeter. Therefore— when the voltage is low, the reading on the voltmeter is nearly zero. As the voltage is increased, the reading showed a slightly increased value. Eventually, the breakdown voltage is reached. At breakdown voltage the reading of the voltmeter showed a sudden jump up to the applied voltage because the internal resistance of the voltmeter is the only high resistance in the loop.

III. RESULTS AND DISCUSSION

(1) Coating

Figure 6 shows the coating around fibers at various heat treatment temperatures (HTT). At HTT of 890°C, the coating was not observable with the optical microscope however x-ray, TEM, and resistivity measurements confirmed that there was a coating on the samples.

Figure 7 shows the distribution of the coating thickness on fibers at various HTT. Figure 8 shows the coating thickness distribution of the cross section of a

FIGURE 6

COATING OF FIBERS AT VARIOUS HTT.

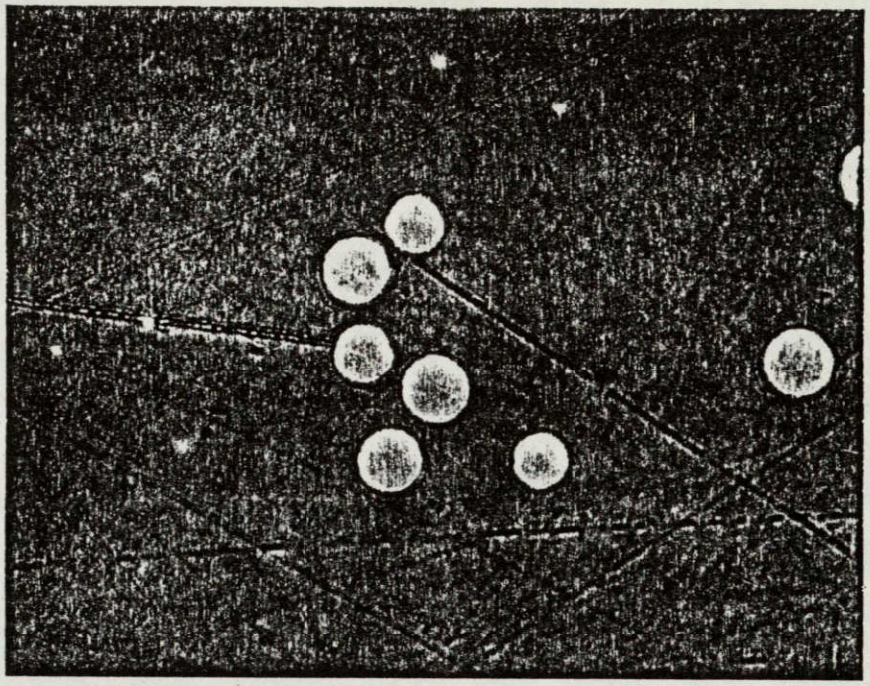

1000 °C (a)

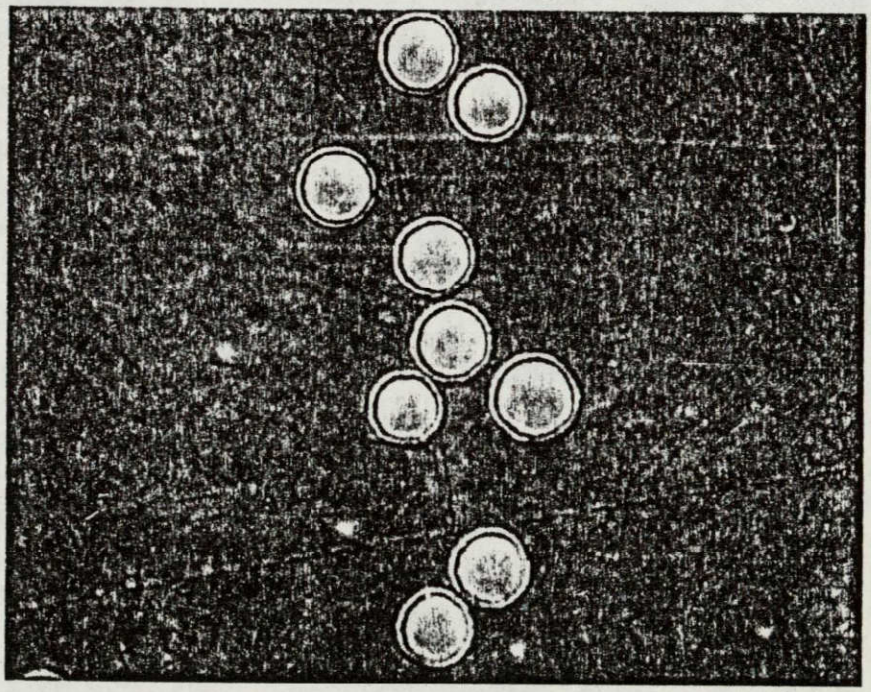

1150 °C (b)

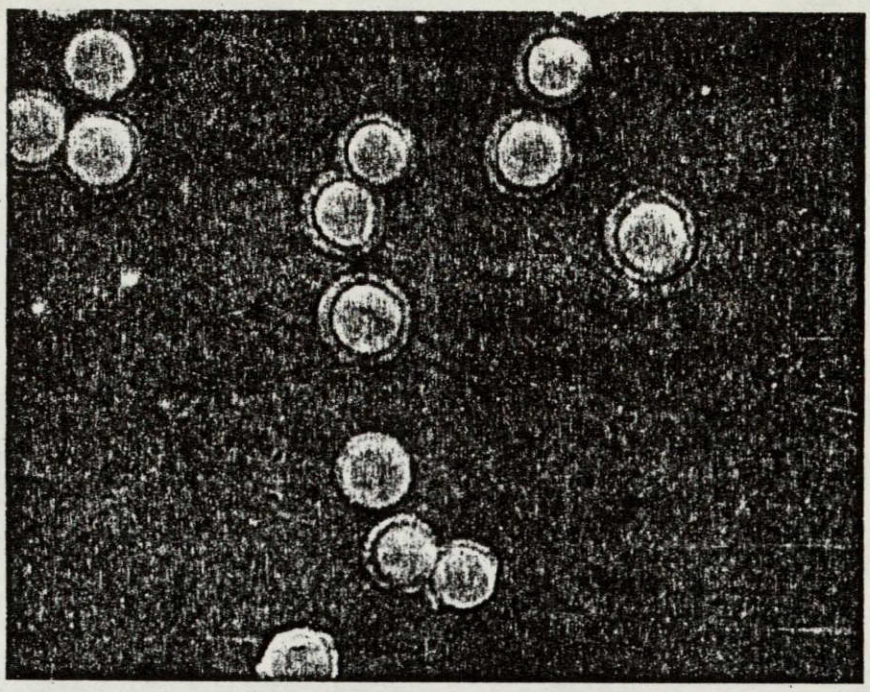

1290 °C (c)

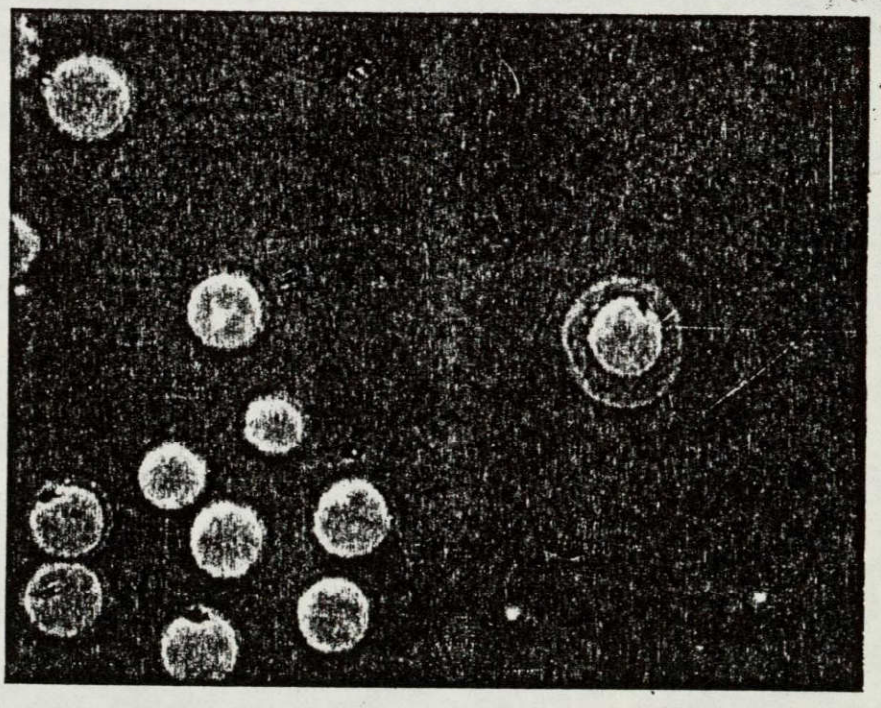

1430 °C (d)

FIGURE 7.

COATING THICKNESS AT VARIOUS HTT.

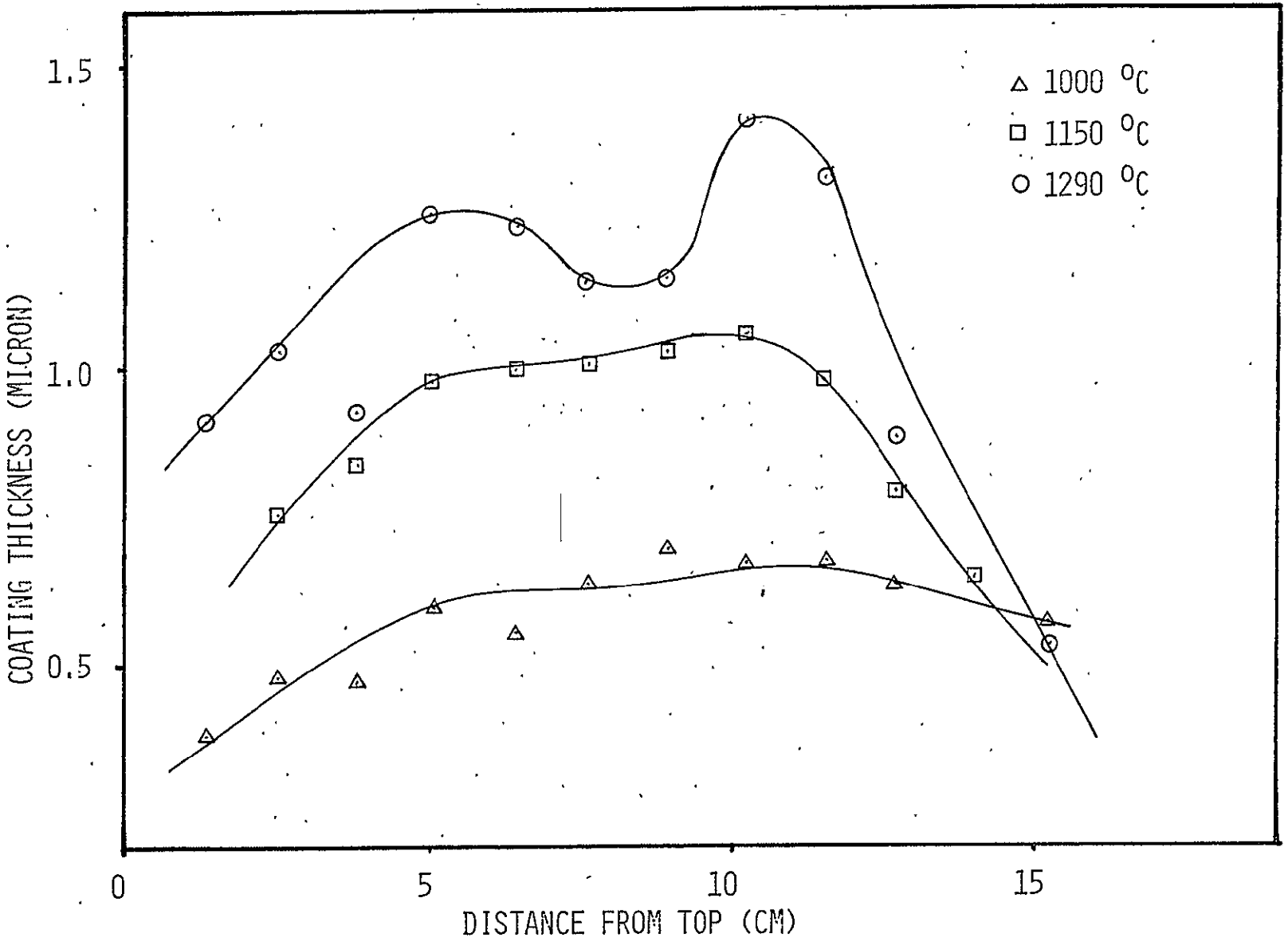
1.5
1.0
0.5
COATING THICKNESS (MICRON)
0
5
10
15
DISTANCE FROM TOP (CM)
△ 1000 °C
□ 1150 °C
○ 1290 °C

FIGURE 8

COATING THICKNESS DISTRIBUTION
OF
THE CROSS SECTION OF A YARN.

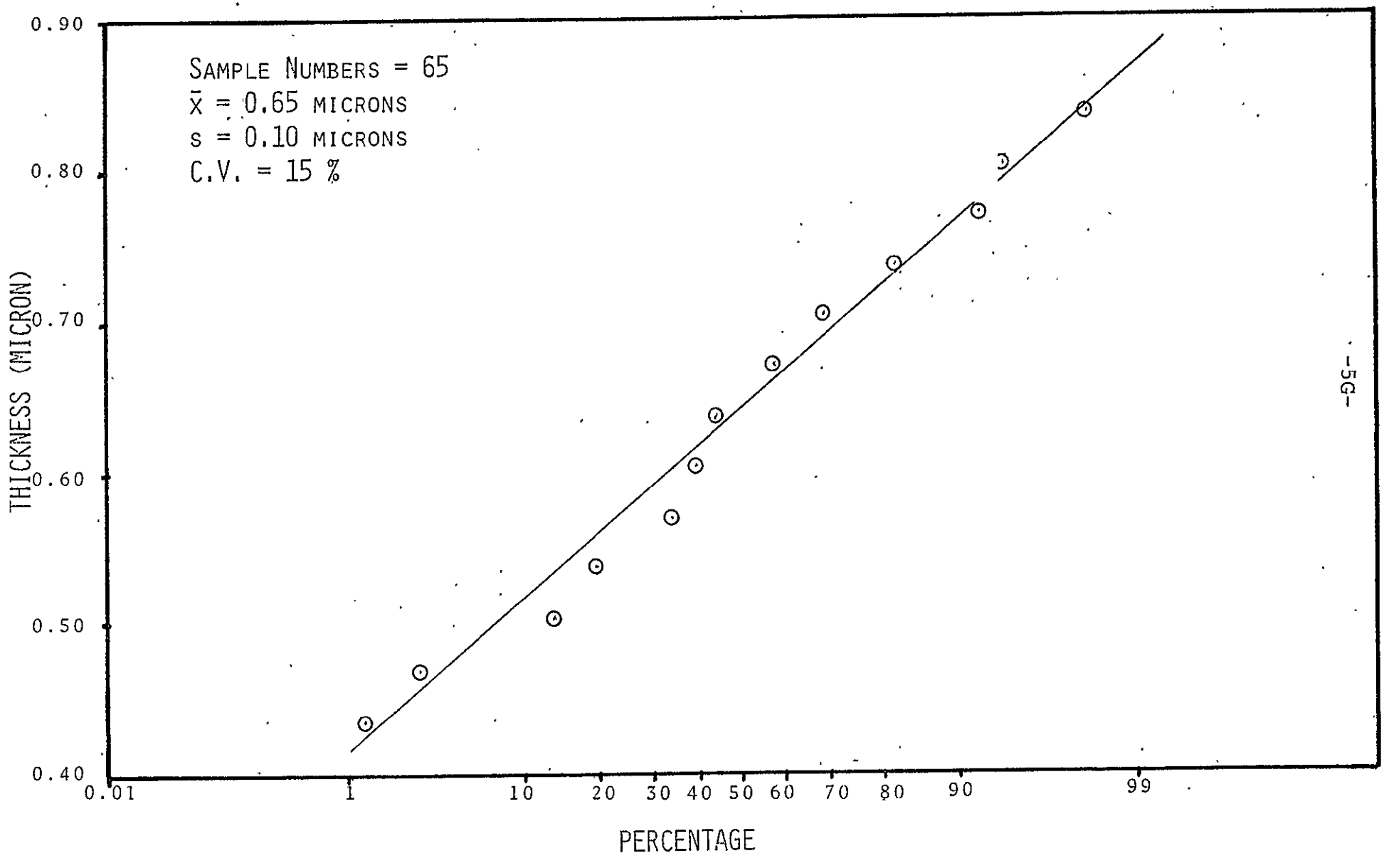
SAMPLE NUMBERS = 65
$\bar{X}$ = 0.65 MICRONS
s = 0.10 MICRONS
C.V. = 15 %
THICKNESS (MICRON)
0.90
0.80
0.70
0.60
0.50
0.40
0.01
1
10
20
30
40
50
60
70
80
90
99
PERCENTAGE

yarn which was heat treated at 1100°C. The sample was taken at 7.54 cm from the top of the furnace. The distribution of the coating thickness is a normal bell shape with the coating thickness varying from 0.45 microns to 0.83 microns. The most important feature of this figure is that the thickness of coating is very uniformly distributed within a narrow range. But with increasing temperature, as can be seen from Fig. 6, the distribution of coating thickness becomes non-uniform. The 1290°C HTT samples (Fig. 6c) show that there is a mixing of samples with thick and thin coatings. The distribution of coating thickness of the samples of 1450°C HTT (Fig. 6d) varied widely from 0.5 microns to 7 microns. Because of the non-uniform geometry of furnace and sample mounting, a certain portion of samples was more exposed to gas flow than other portions. The wide fluctuation in thickness of coating at higher HTT samples may be caused by the following condition. At the beginning of the coating process there exists enough space between fibers within a bundle to allow gas flow but with increasing time or reaction rate (high HTT) the outside portion of a bundle (more exposed to gas) reacts more than the inner fibers (less exposed to gas). Eventually the outside fibers of the bundle grow thick enough to prevent gas flow to the inner fibers. Hence, the coating thickness of inner fibers is about constant even with increasing reaction time. The same phenomenon can be found at lower HTT with longer reaction time. The thickness

distribution of samples at 1150°C HTT for 60 seconds is very similar to that at 1290°C which was treated for 30 seconds. Figures 7 and 9 can be explained within the same context. At lower HTT or shorter time, the curves of the figures are flatter than those at higher HTT or longer time. This means that fibers can be coated uniformly at low reaction rates. The thin coating thickness still means relatively short times, however.

Figure 9 shows the thickness of coating distribution along each sample, from top to 15 cm down the furnace tube, for various reaction times at 1150°C HTT. Figure 10 shows the difference between Hercules AS-1 and Fortafil 4R. The variation in Hercules AS may be caused by false twist or other differences in tow characteristics. Figure 11 shows the thickness distribution at various gas flow rates. Figure 12 shows the thickness distribution of different processes, i.e. NH_3 1st or BCl_3 1st. Since the furnace was purged with N_2 gas, it can be supposed that from the above figures (Figs. 11 and 12), the thickness of coating is proportional to the BCl_3 gas flow rate.

(2) Structure of Coating

From the results of x-ray diffraction patterns, BN and B_4C were identified in all samples. The x-ray analysis also shows the BN structure is hexagonal.

FIGURE 9

COATING THICKNESS DISTRIBUTION
AT
VARIOUS REACTION TIME AT 1150°C HTT.

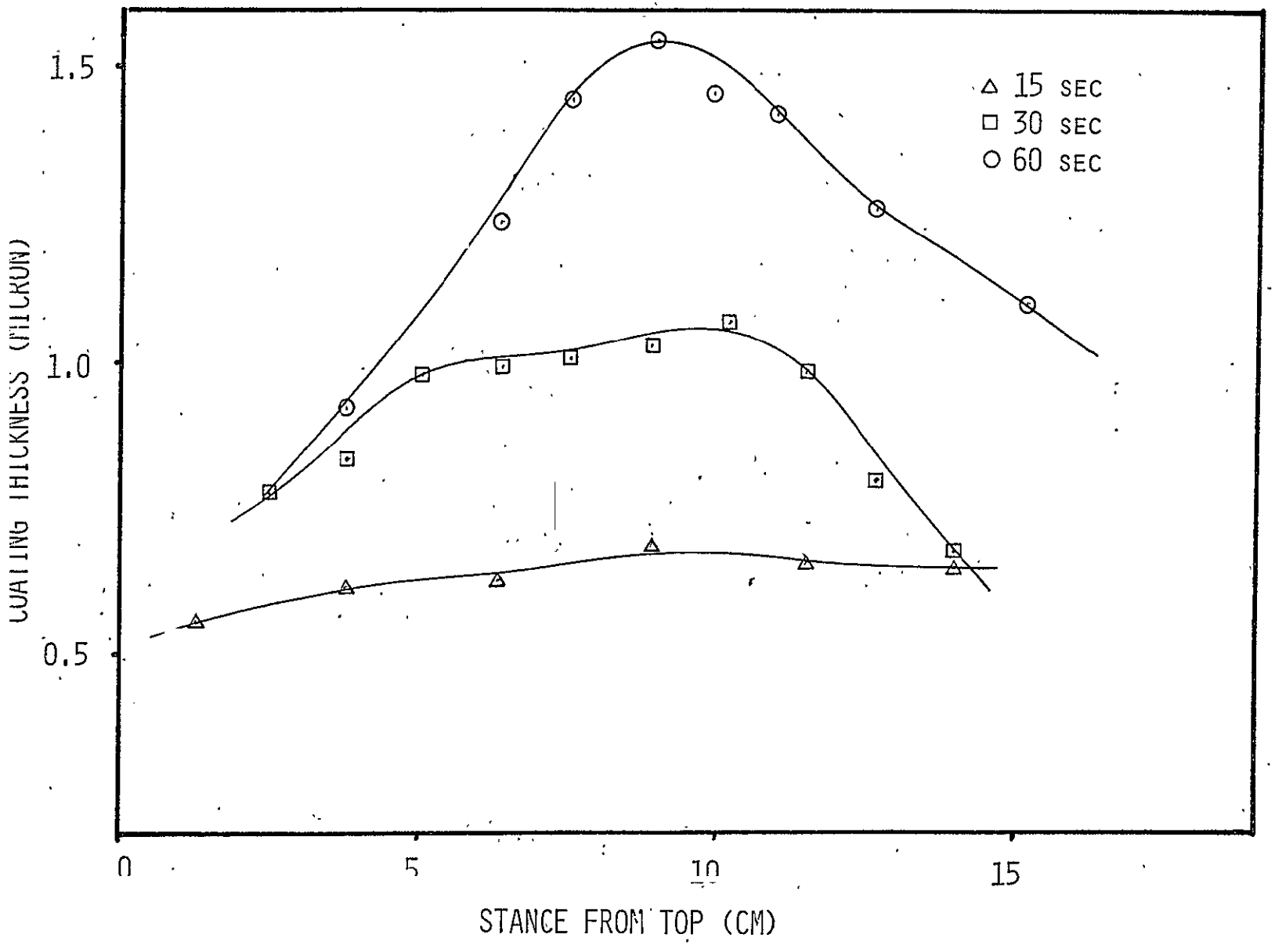
COATING THICKNESS (THICKUN)
1.5
1.0
0.5
0
5
10
15
STANCE FROM TOP (CM)
15 SEC
30 SEC
60 SEC

FIGURE 10

COATING THICKNESS DISTRIBUTION
OF
FORTAFIL 4R AND HERCULES AS-1.

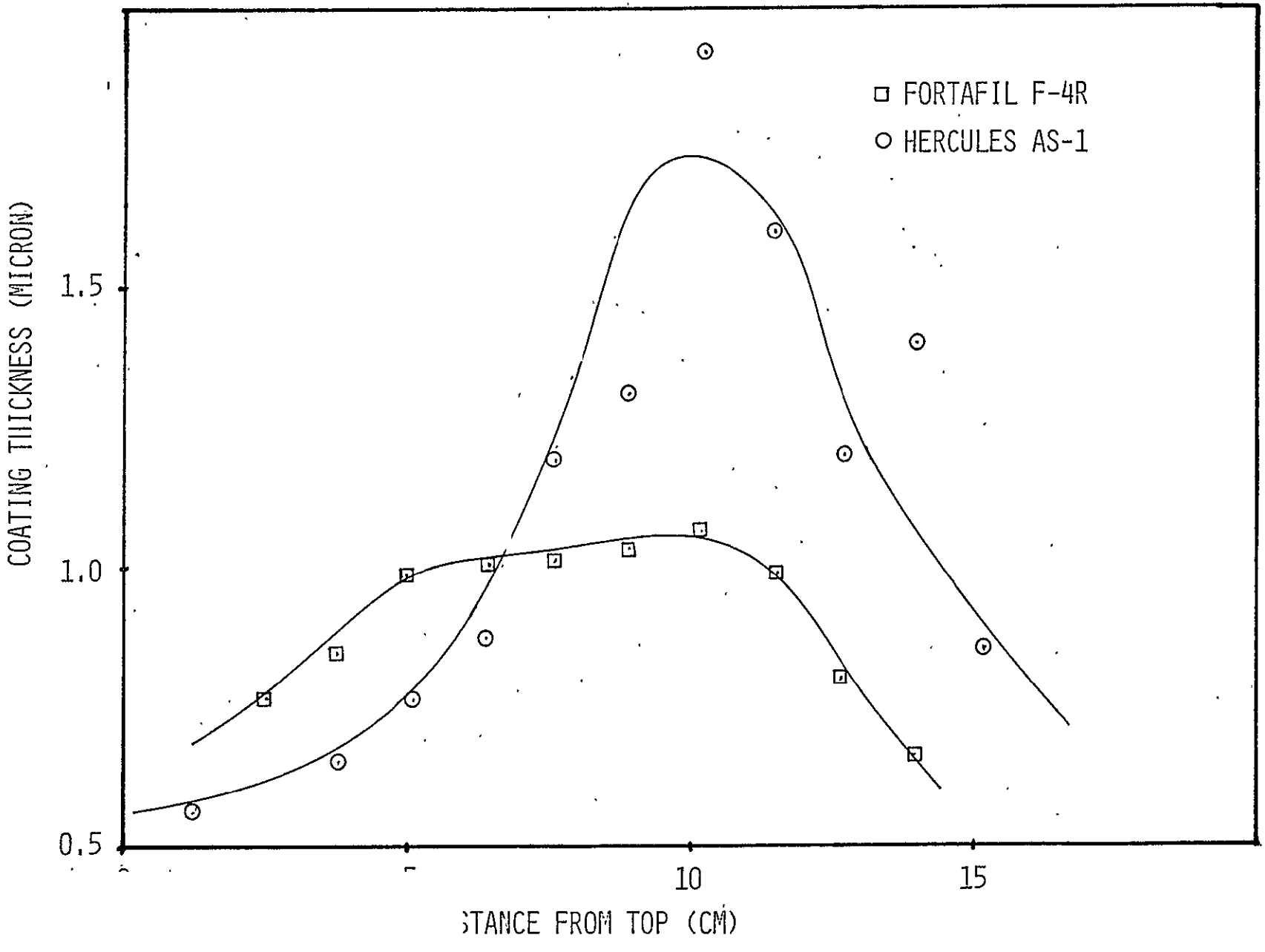
FORTAFIL F-4R
HERCULES AS-1
COATING THICKNESS (MICRON)
1.5
1.0
0.5
10
15
STANCE FROM TOP (CM)

FIGURE 11

COATING THICKNESS DISTRIBUTION
AT
VARIOUS GAS FLOW RATES.

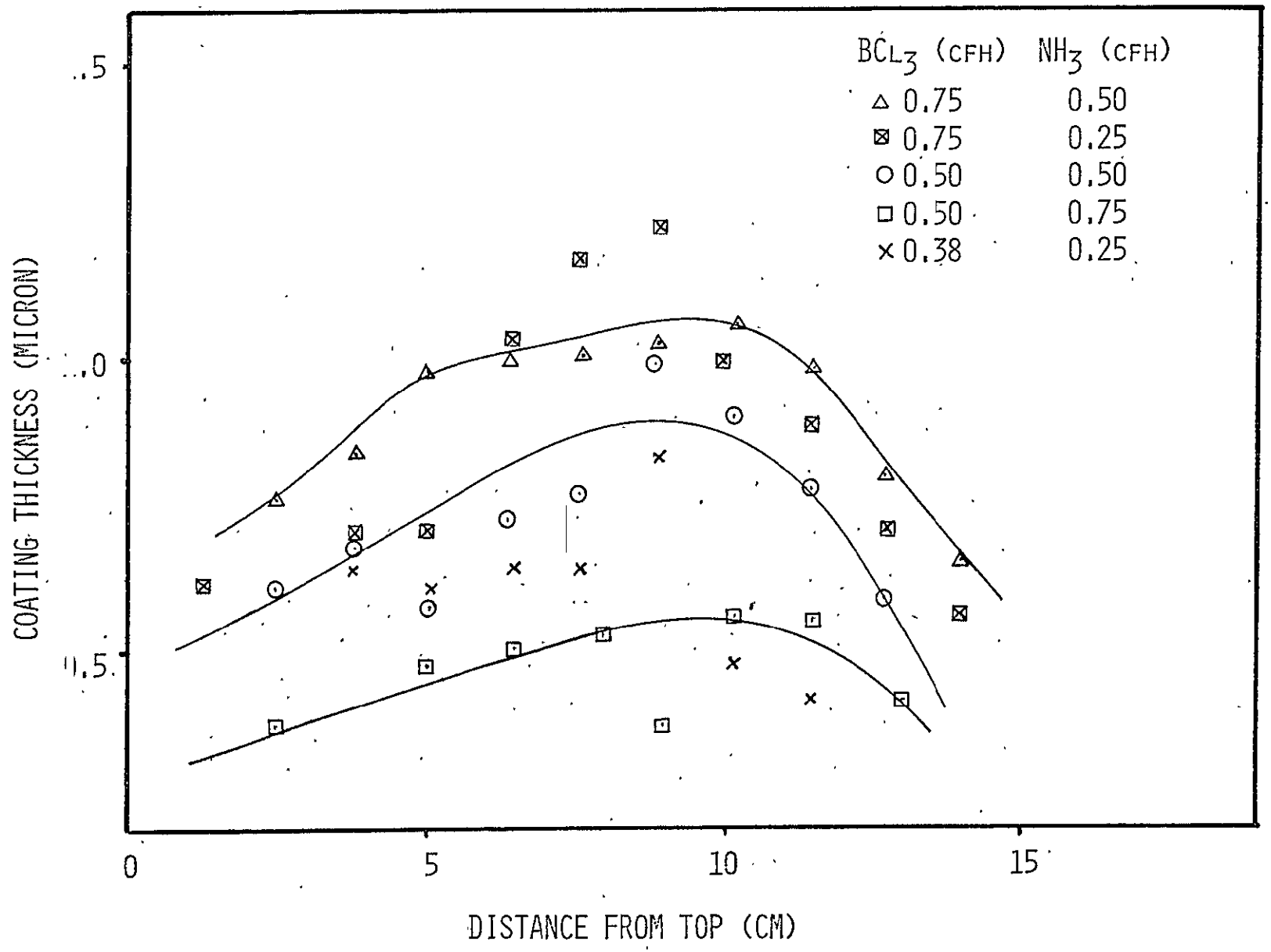
BCL_3 (CFH) NH_3 (CFH)
△ 0.75 0.50
⊠ 0.75 0.25
○ 0.50 0.50
□ 0.50 0.75
× 0.38 0.25
.5
1.0
1.5
COATING THICKNESS (MICRON)
0
5
10
15
DISTANCE FROM TOP (CM)

FIGURE 12

COATING THICKNESS DISTRIBUTION
WITH
DIFFERENT PROCESSES.

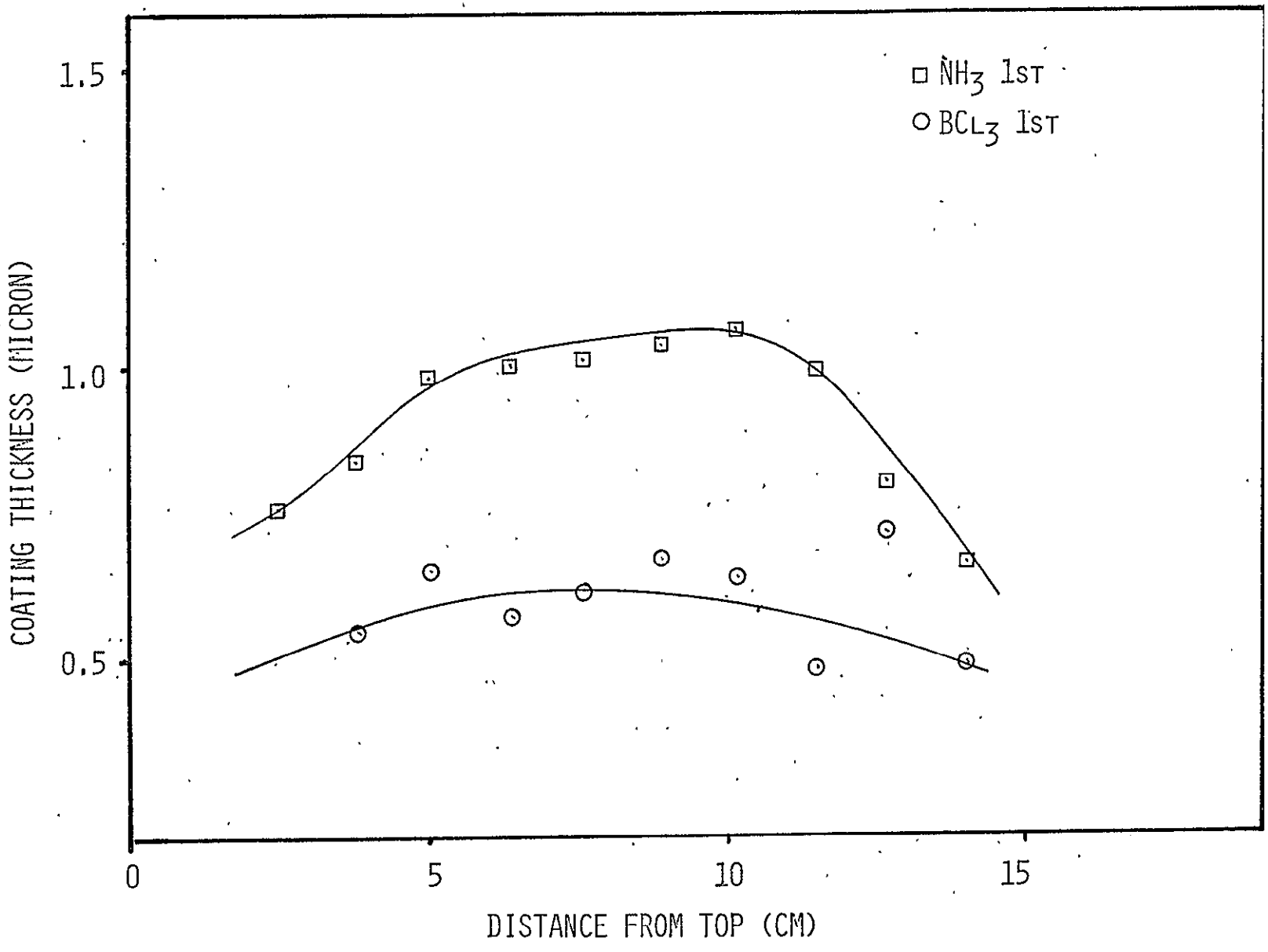
□ NH3 1ST
○ BCL3 1ST
COATING THICKNESS (MICRON)
1.5
1.0
0.5
0
5
10
15
DISTANCE FROM TOP (CM)

Since the spacing of the (0002) plane of graphite (d = 3.36 Å) is similar to that of BN, the dark field image was used to identify electron diffraction patterns which were taken with TEM. Figure 13 shows an electron diffraction pattern and (0002) dark field image at 1150°C HTT. Table II shows the radius of each diffraction ring which was measured and identified at different HTT. The data is consistent with (BN)4H hexagonal structure, except for the first (0002) ring. As HTT increased, the d spacing gradually decreased from 3.58 Å to 3.34 Å. Since the reference (BN)4H structure was obtained by heating BN to 2050°C, the spacing is smaller than all of our data. Figure 14 shows an electron diffraction pattern with preferred orientation (dark field image from BN coating deposited at 1430°C).

From x-ray and TEM results one might postulate that B_4C layer only existed between BN and carbon fiber and B_4C layer forms a better bond to the fiber than BN coating. Also, perhaps the B_4C layer was produced as boron atoms diffused into the carbon fiber.

Figure 15 shows the coating of a fiber photographed with SEM. Figure 16 shows the cross section of one of the thickest coated fibers (1430 °C HTT). From Fig. 16 it can be seen that the coating grew radially from the center to the outside with the characteristic CVD growth cone microstructure.

FIGURE 13

ELECTRON DIFFRACTION PATTERN
AND
(0002) DARK FIELD IMAGE AT 1150°C HTT.

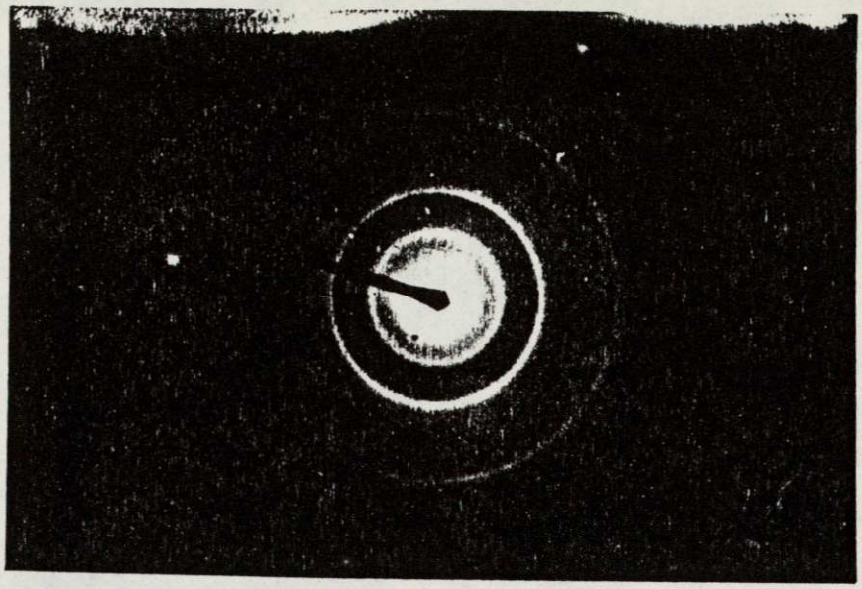

x 1.22

BN Coating

Carbon fiber

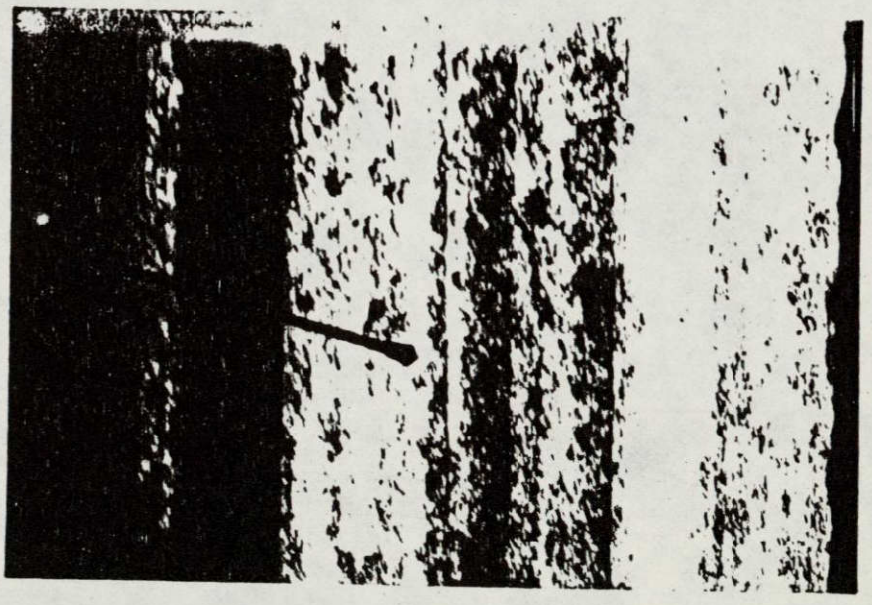

1 μm

FIGURE 14

ELECTRON DIFFRACTION PATTERN
WITH
PREFERRED ORIENTATION
AND
(0002) DARK FIELD IMAGE FROM BN COATING
TREATED AT 1430°C.

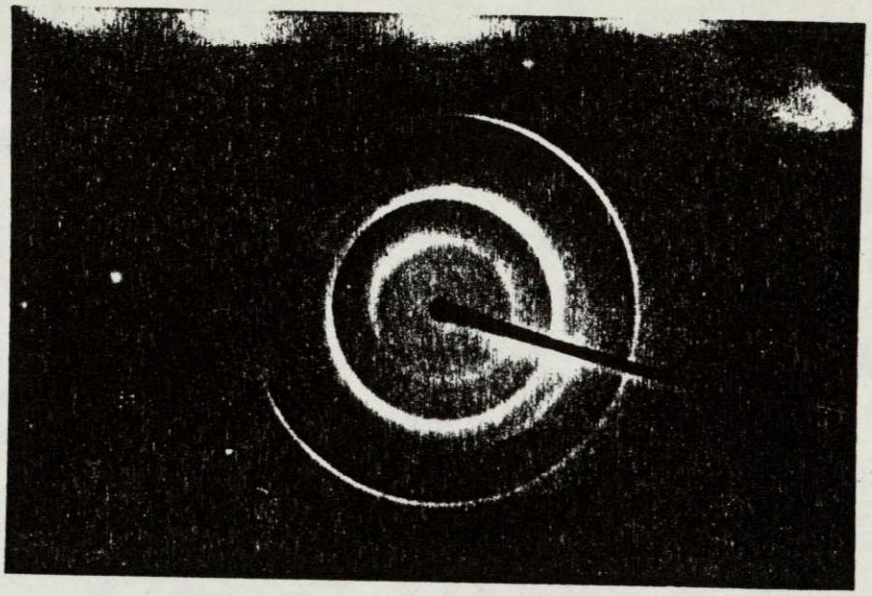

x 1.22

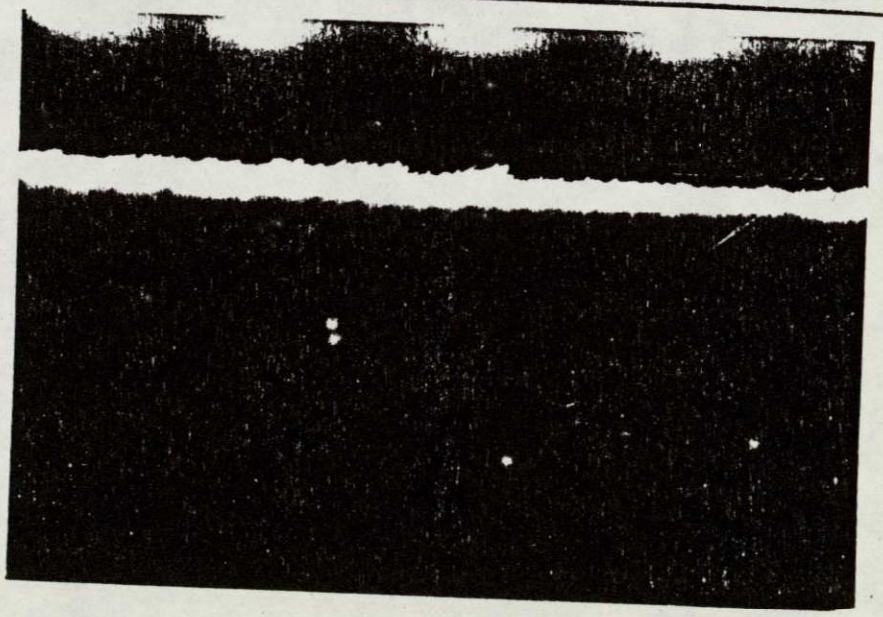

FIGURE 15

COATING OF FIBER (BY SEM).

(middle)

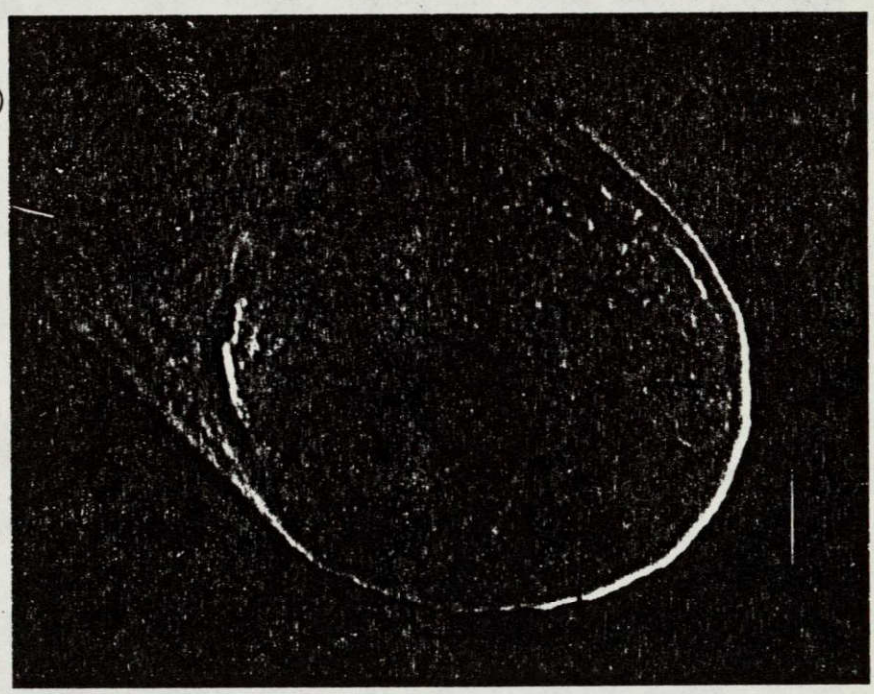

1 μm

FIGURE 16

CROSS SECTION OF COATED FIBER
WITH
POLARIZED LIGHT.

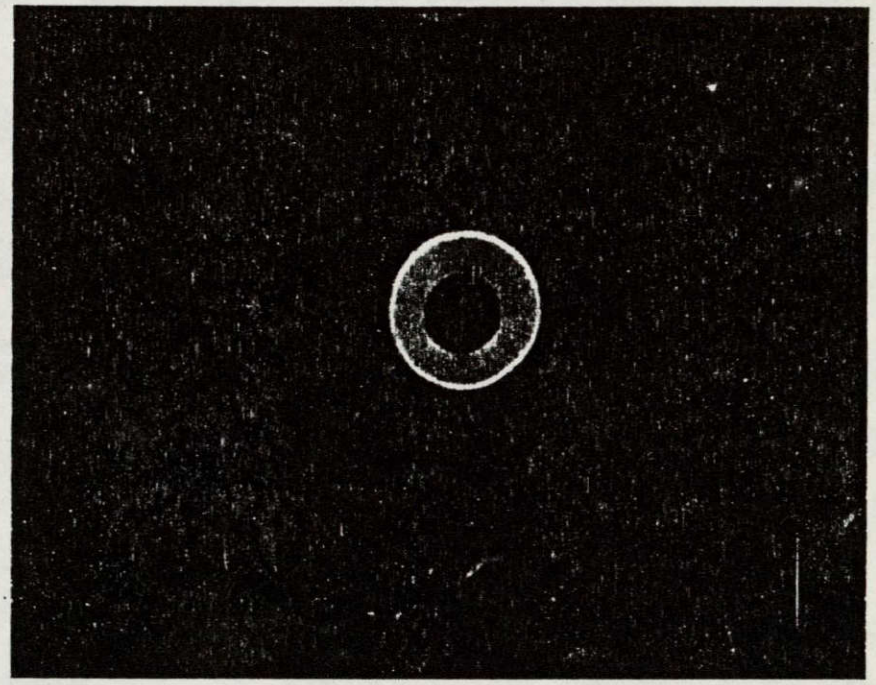

TABLE II

THE RADIUS OF DIFFRACTION PATTERNS

hkl	2050 °C*	1430 °C	1290 °C	1150 °C	1000 °C	885 °C
002	3.33	3.35	3.46	3.53	3.53	3.58
100	2.17	2.10	2.13	2.11	2.09	2.13
110	1.25	1.22	1.22	1.23	1.23	1.25

Standard BN

All units are angstrom.

Electron diffraction results show that the BN coating became progressively more crystalline and oriented along the fiber axis as HTT was increased from 885°C to 1430°C. Figure 18 shows pictures of different HTT samples under polarized light. An observation is that the coating is more birefringant (brighter) with increasing HTT. The birefringance of the polarized light pictures of the coating agrees well with the TEM results showing a decrease in d spacing at higher HTT.

(3) Electrical Properties

(A) Resistivity

By shielding the electric circuit to reduce noise, the current measurement capacity of the electrometer used was about 10^{-9} amps. With 10 volts applied by the DC power supply, all samples allowed passage of a current less than 10^{-9} amps, i.e. the resistance of the coating was higher than 10^{10} ohms. The resistivity of the BN coating is higher than 10^{9} ohm-meter which was calculated with the following equation (derivation is shown in Appendix A):

$$\rho = \frac{2\pi RL}{\ell n D_o/D_i} \qquad (1)$$

where ρ; the resistivity of the BN coat

R; resistance,

ℓ; the length of BN contact with silver paint,

D_i; the inside diameter of the BN coating and,

D_o; the outside diameter of the BN coating.

The resistivity of the BN coating was also measured by a voltmeter (Fig. 4b). When the 10 volt potential was applied, the reading of the voltmeter showed less than 0.0001 volts. Since the current passed through the coating and voltmeter is the same, the following equation can be derived:

$$\frac{R}{R_i} = \frac{10 - V}{V} \qquad (2)$$

where R_i is the internal resistance of the BN coating and V is the reading of the voltmeter. Using Eq. 2 the resistivity of the coating was calculated to be more than 10^{10} ohm-meter.

From the above results it can be concluded that the resistivity of the BN coating is more than 10^9 ohm-meter.

(B) Breakdown Voltage

The breakdown voltage of BN coating is shown in Table III. All the samples were taken from the same position in the furnace (7.62 cm from the top of the furnace). The samples at 1290°C HTT show a significantly higher value of breakdown voltage than other samples.

It is supposed that the hottest zone of the furnace is in the range between 7.54 cm and 10 cm. The temperatures reported for all our samples are at the hottest zone. Figure 17 shows the breakdown voltage at various HTT along the sample length. From this figure, by comparing 1290°C

TABLE III

THE BREAKDOWN VOLTAGE OF BN COATING

HTT (^{o}C)	Time (Second)	Flow Rate (cfh) BCl_3	Flow Rate (cfh) NH_3	Breakdown Voltage (volt/micron)
885	30	0.75	0.50	*1
1000	30	0.75	0.50	571
1150	30	0.75	0.50	518
1290	30	0.75	0.50	967
1430	30	0.75	0.50	561*2
1150	15	0.75	0.50	457
1150	60	0.75	0.50	477
1150	30	0.75	0.50	340 BCl_3 1st
1150	30	0.50	0.50	468
1150	30	0.50	0.75	444
1150	30	0.38	0.25	625
1150	30	0.25	0.75	340
1150	30	0.75	0.25	512
1150	30	0.75	0.50	648 Hercules As-1

*1; The breakdown voltage was about 60 volts.

*2; The breakdown voltage of thinly coated fibers.

FIGURE 17

BREAKDOWN VOLTAGE AT VARIOUS HTT.

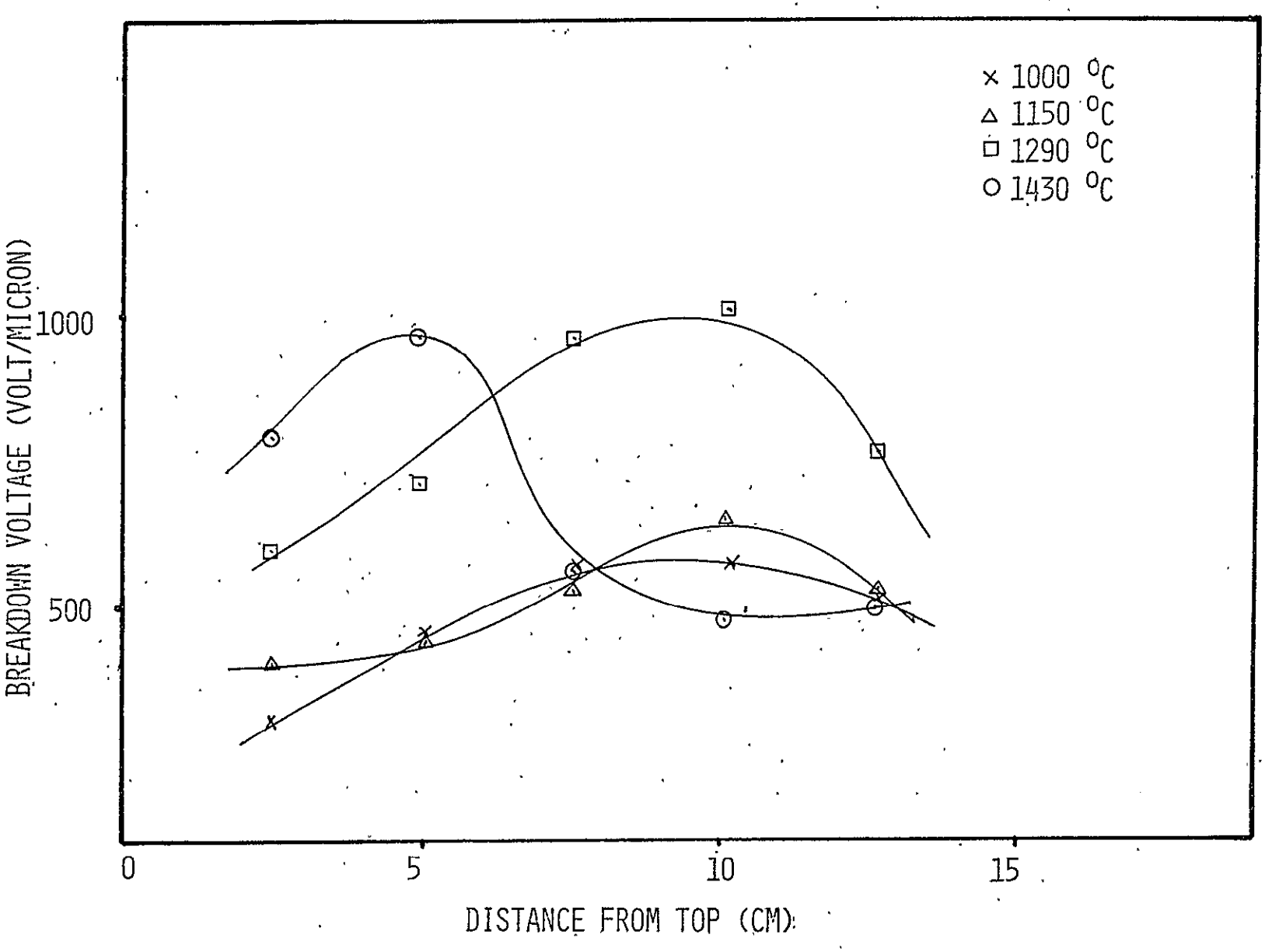
× 1000 °C
△ 1150 °C
□ 1290 °C
○ 1430 °C
BREAKDOWN VOLTAGE (VOLT/MICRON)
1000
500
0
5
10
15
DISTANCE FROM TOP (CM)

FIGURE 18

COATING OF FIBER WITH POLARIZED LIGHT.

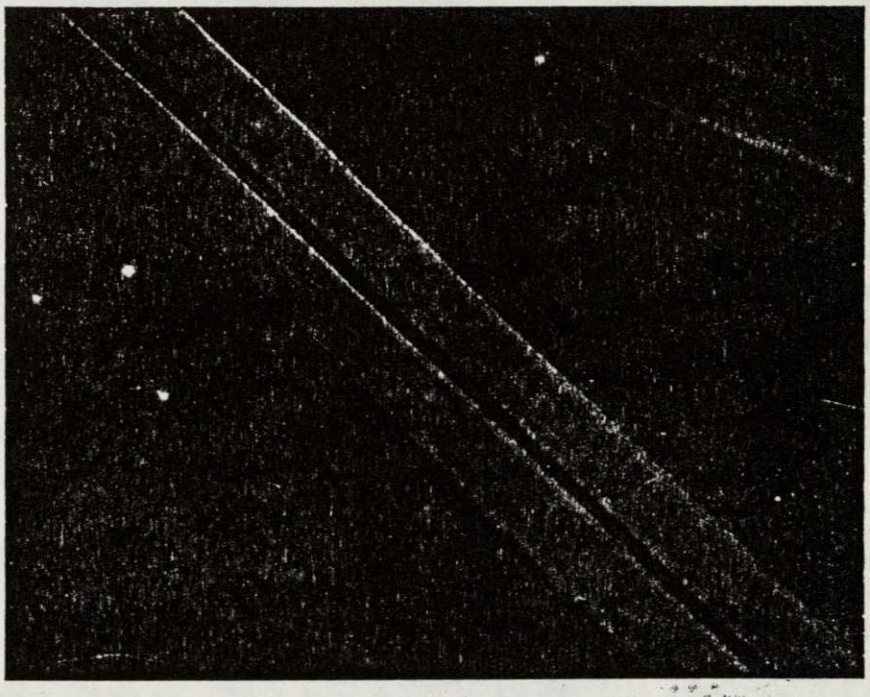

1000 °C (a)

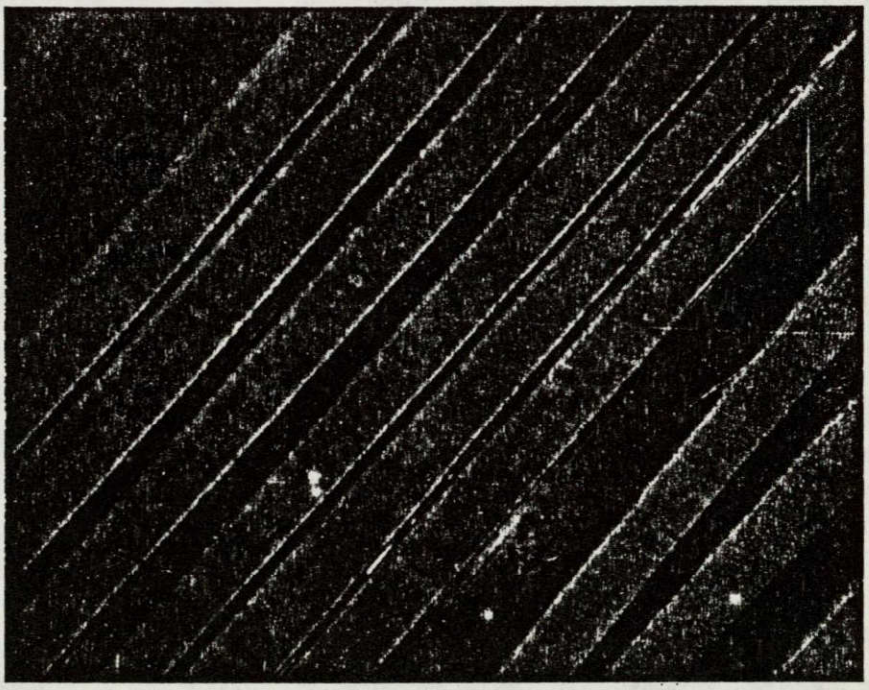

1150 °C (b)

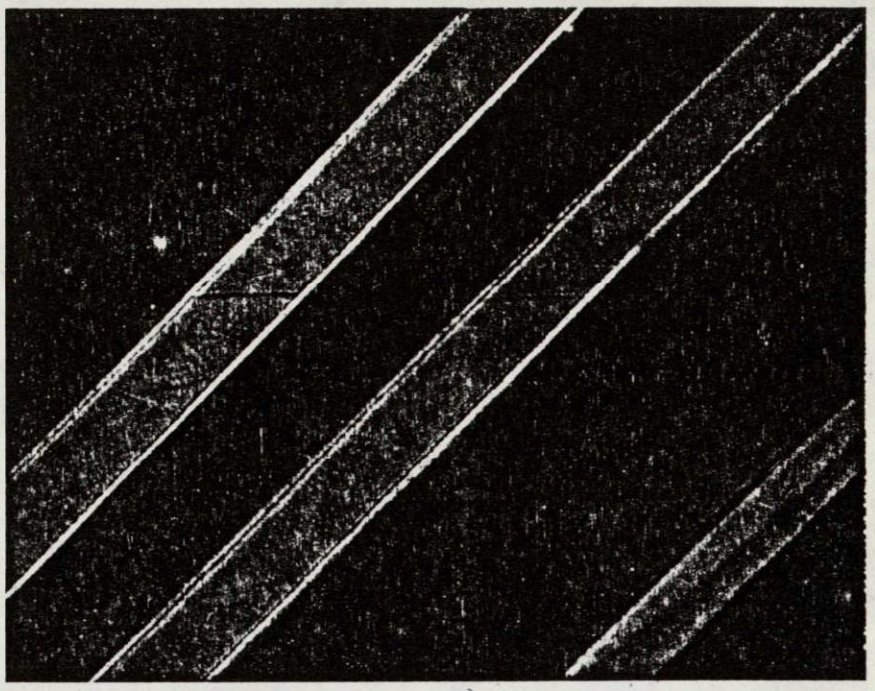

10 μm

1290 °C (c)

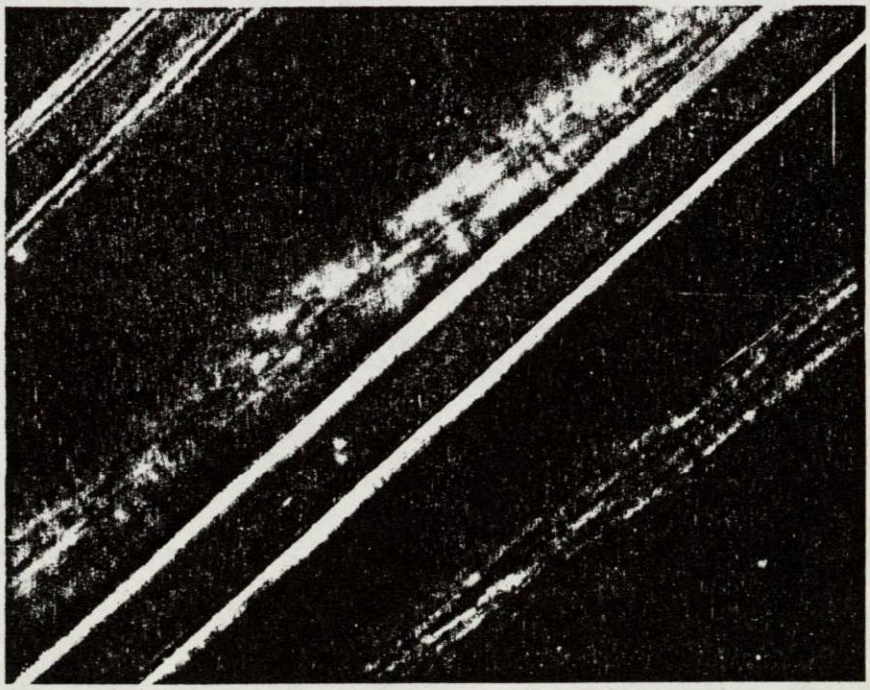

10 μm

1450 °C (d)

HTT and 1450°C HTT, it can be postulated that about 1300°C HTT is the proper temperature to achieve the highest breakdown voltage per unit width of thickness under the present conditions.

The measurement of density of coating, by using a density column, shows that the density of 1290°C HTT is higher than those of other samples. Table IV shows that the change of density accompanied the change of breakdown voltage at various HTT. However, the maximum density achieved is significantly below theoretical, and better properties can be expected in the future.

(4) Mechanical Properties

The modulus of coated fiber is always less than that of uncoated fiber. Neglecting the thickness of coating, the modulus of coated fibers is equal to that of uncoated fibers. BN, with a low preferred orientation, has a much higher thermal expansion coefficient (7.51×10^{-6} 1/°C) than that of carbon (0.66×10^{-6} 1/°C). When coated carbon fibers are cooled down, the BN coating has tensile residual stress and the carbon fiber has compressive stress. During a tensile test the BN coating is observed to crack in several points along one fiber. Since the BN coating failed, only the central carbon fiber is tested in tension. A coating with a higher preferred orientation would both minimize the residual stress and loss in modulus

TABLE IV

DENSITY AND BREAKDOWN VOLTAGE VS. HT

	1150 °C	1290 °C	1430 °C
Breakdown Voltage (volt/micron)	518	967	561
Density (gm/cc)	1.684	1.80	1.687

IV. DEVELOPMENT OF X-RAY DIFFRACTION TECHNIQUES FOR THE MEASUREMENT OF PREFERRED ORIENTATION

The strong correlation of carbon fiber modulus with preferred orientation of crystalline fibrils within the fiber makes accurate methods of measuring preferred orientation essential, especially where direct modulus measurements can not be performed. X-ray diffraction measurements of the preferred orientation of a particular set of crystal planes can be made by examining the same reflection from different angles. This can be done for carbon fibers by rotating the fiber axis about a rotation axis coincident with the plane defined by the incident and diffracted beams as shown in Fig. 19. The variation of diffracted peak intensity as a function of the fiber rotation angle ϕ can be used as a measure of preferred orientation. The present experimental work compares two methods of measuring the diffracted x-ray intensity: one quick and approximate and the other time-consuming and accurate.

In the quick procedure the goniometer of the x-ray diffractometer is set to the exact Bragg angle and the intensity through the final slit is measured as a function of rotation angle ϕ. Figure 20 shows a schematic diagram of such a plot. The narrower the resulting maxima, measured at half height, the greater the preferred orientation.

FIGURE 19

EXPERIMENTAL SETUP FOR ROTATION OF FIBER IN X-RAY BEAM.

FIGURE 20

TYPICAL CHART RECORDING OF PEAK HEIGHT vs. ϕ.

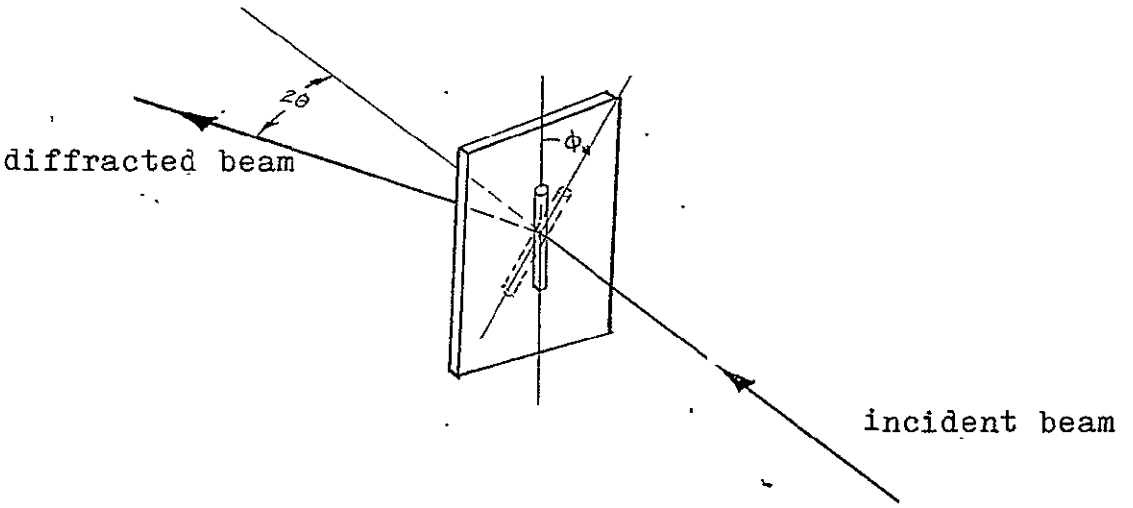
2θ
diffracted beam
Φ
incident beam

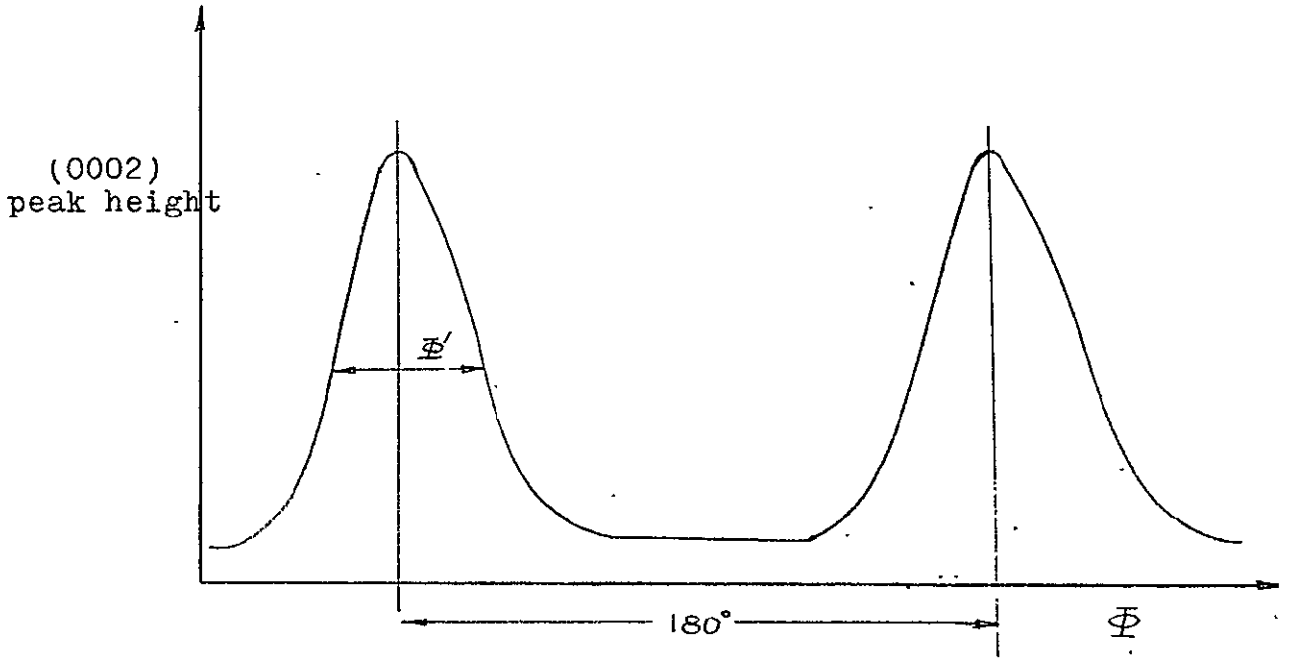
(0002)
peak height
Φ'
180°
Φ

However, peak heights are only an approximation to the intensity diffracted by a set of planes. The total intensity diffracted is the integrated intensity measured as the area under the 2θ curve of the x-ray peak. For the determination of preferred orientation using integrated intensity, a 2θ scan must be run for many discrete values of the fiber rotation angle ϕ. This is a very time-consuming process and has been neglected in favor of the more rapid continuous measurement of peak heights.

To compare the accuracy of the peak height and integrated intensity methods, the same fibers were measured by both methods. The results were compared by normalizing intensity values at each ϕ to that for $\phi = 0°$. Intensity versus 2θ curves are shown in Figs. 21, 22, and 23 for (0002) peaks of pitch, Hercules HMS and Hercules AS fibers, respectively. The "d" spacings quoted for the three fibers directly calculated (uncorrected) from the data. The areas under these curves were measured, normalized to the curve for $\phi = 0°$, and compared with the results from the peak height method in Figs. 24, 25, and 26 for pitch, HMS, and AS fibers, respectively.

The full widths at half maximum for each method are summarized in Table V. The usual corrections for instrumental broadening and fiber misalignment were assumed the same for each method and ignored in these comparisons. These

FIGURE 21

PITCH FIBER - DIFFRACTION INTENSITY PROFILES
FOR ø SETTINGS OF 0°, 5°, 10°, 15°,
AND 25°.

Pitch fiber

$2\theta_B = 25.85°$

$d_{0002} = 3.44$ Å

Φ	Area ratio
0°	1
5°	0.756
10°	0.410
15°	0.186
20°	0.091
25°	0.034

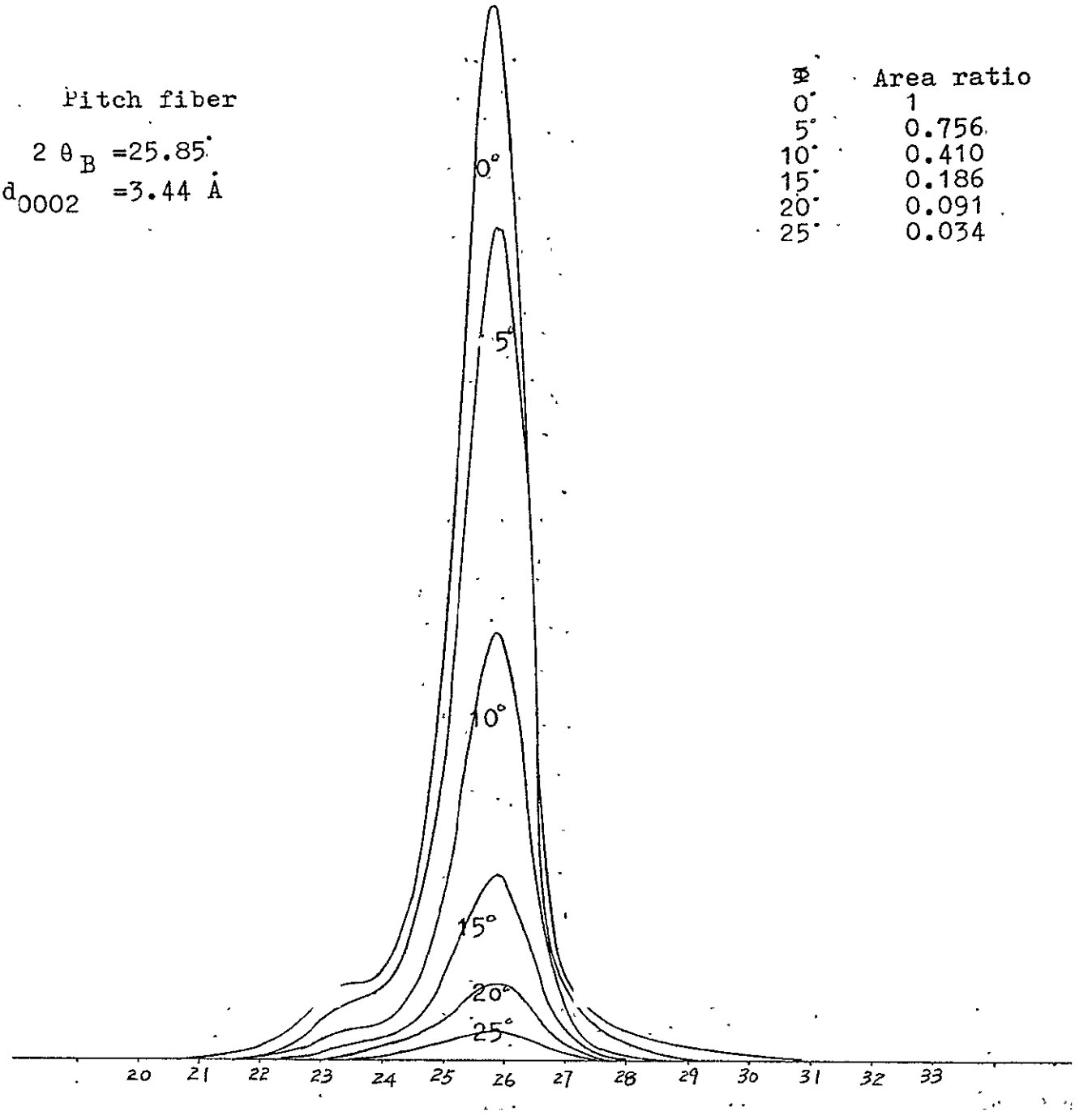

FIGURE 22

HERCULES HMS FIBER - DIFFRACTION INTENSITY PROFILES FOR ø SETTINGS OF 0°, 5°, 10°, 15°, 25°, AND 30°.

Hercules HMS fiber

$2\theta_B = 25.70^\circ$

$d_{0002} = 3.46$ Å

Φ	Area ratio
0°	1
5°	0.820
10°	0.565
15°	0.323
20°	0.195
25°	0.086
30°	0.050

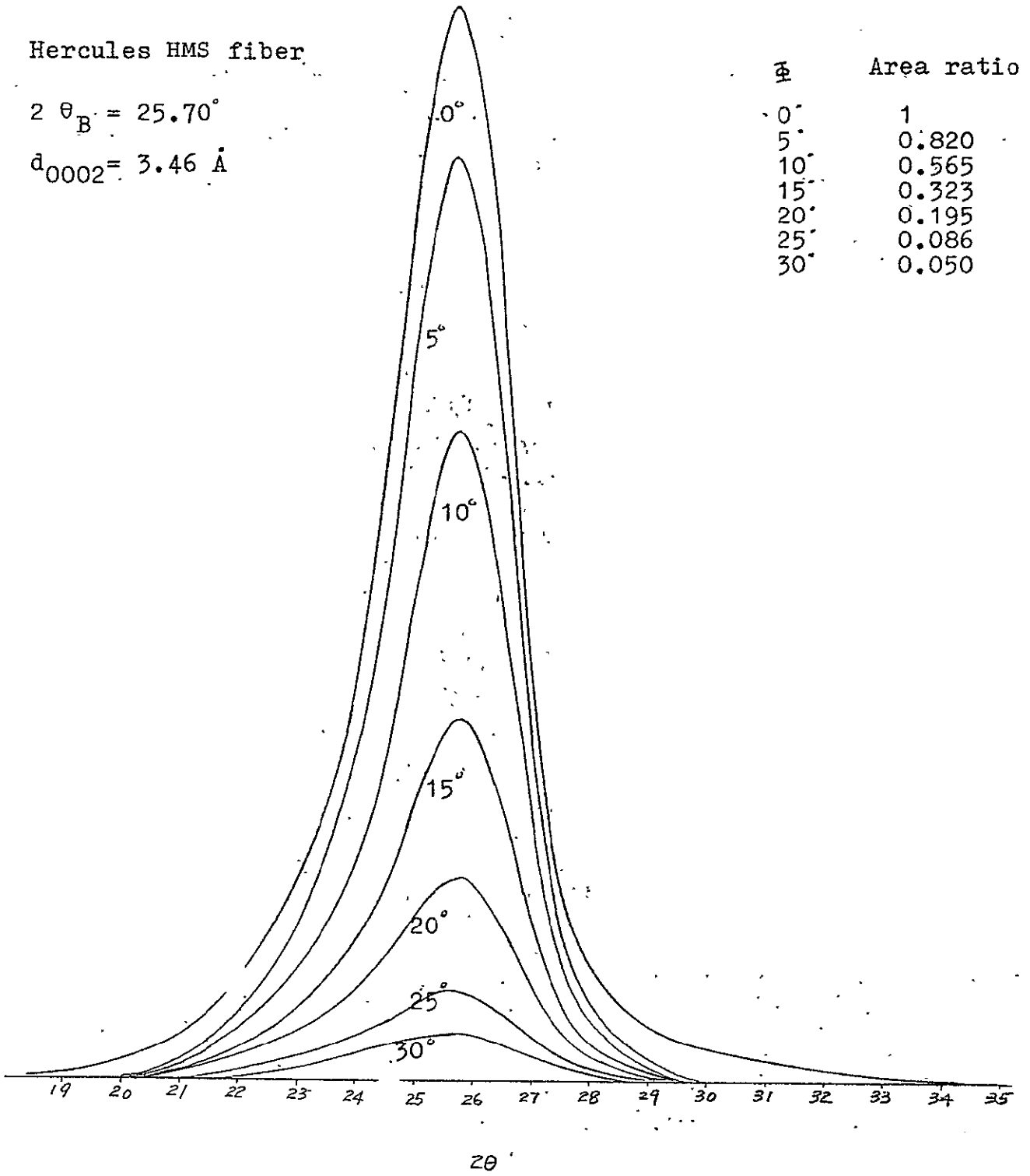

FIGURE 23

HERCULES AS FIBER - DIFFRACTION PROFILES FOR ø SETTINGS OF 0°, 5°, 10°, 15°, 25°, 30°, AND 35°.

Hercules AS fiber

$2\theta_B = 25.30^\circ$

$d_{0002} = 3.52$ Å

Φ	Area ratio
0°	1
5°	0.941
10°	0.815
15°	0.626
20°	0.434
25°	0.259
30°	0.150
35°	0.089

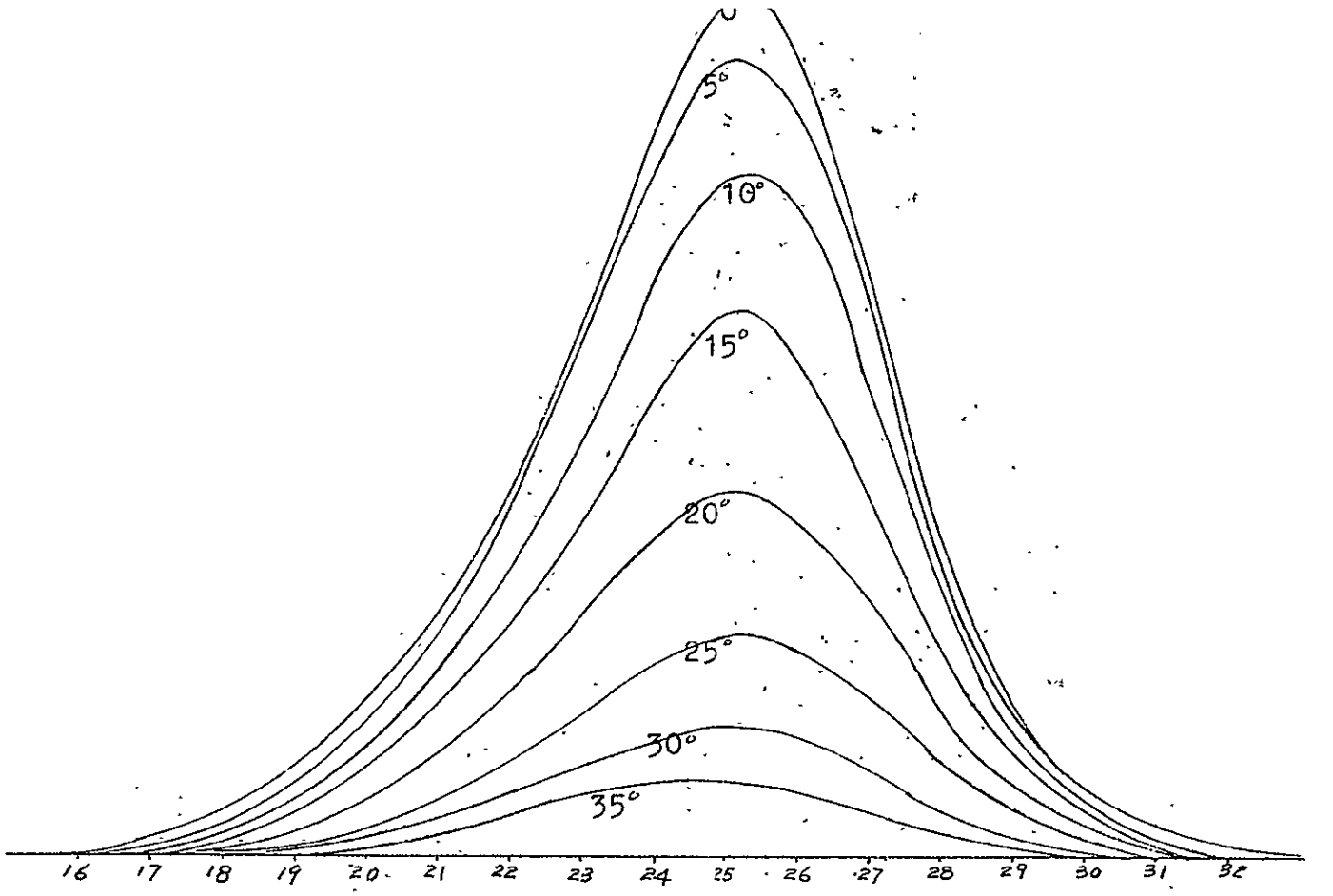

FIGURE 24

PITCH FIBER - COMPARISON OF PEAK HEIGHT VS. INTEGRATED INTENSITY (FROM FIG. 21) FOR PREFERRED ORIENTATION EVALUATION.

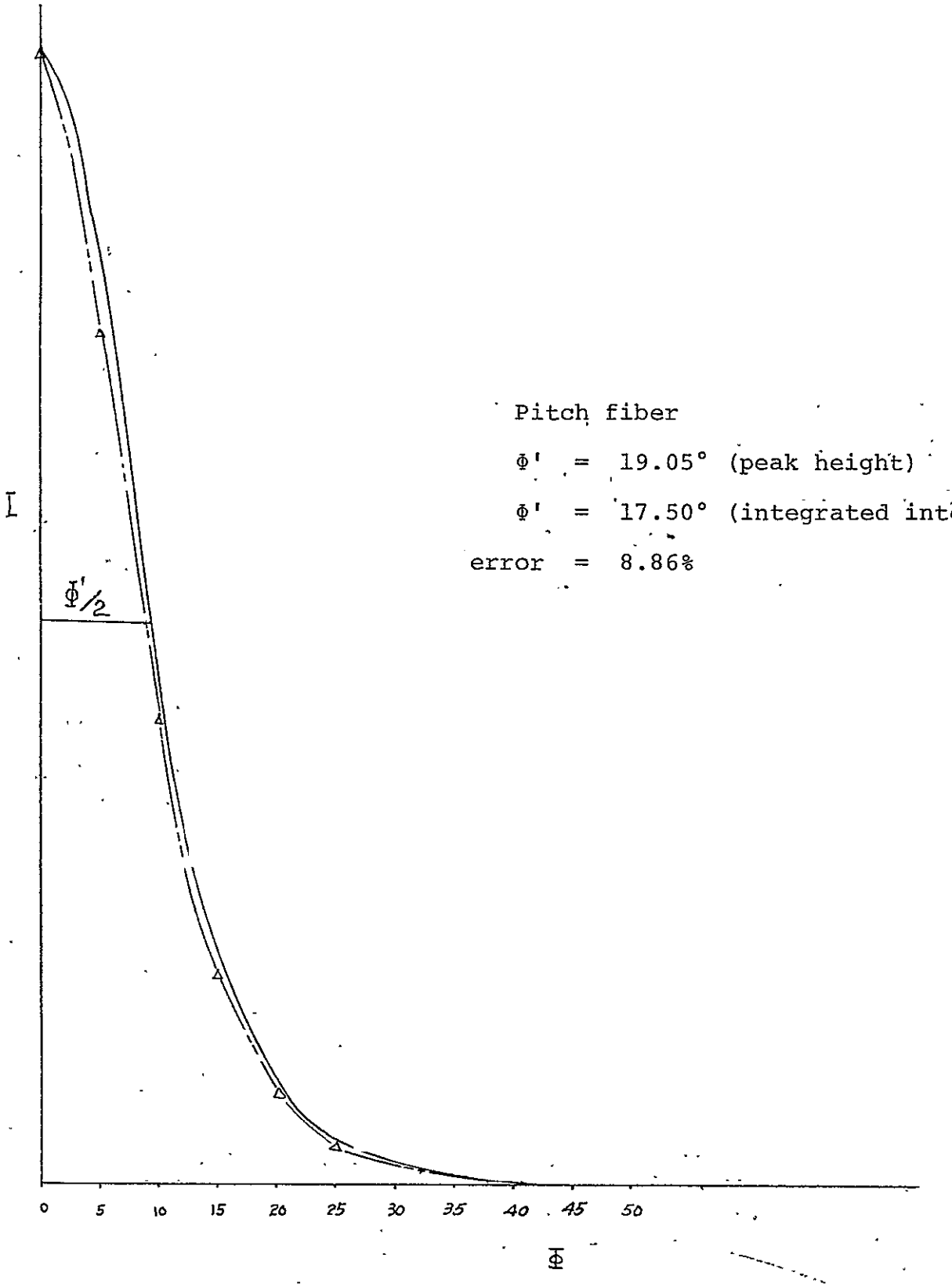

Pitch fiber

Φ' = 19.05° (peak height)

Φ' = 17.50° (integrated intensity)

error = 8.86%

FIGURE 25

HERCULES HMS FIBER - COMPARISON OF PEAK HEIGHTS vs. INTEGRATED INTENSITY (FROM FIG. 22) FOR PREFERRED ORIENTATION EVALUATION.

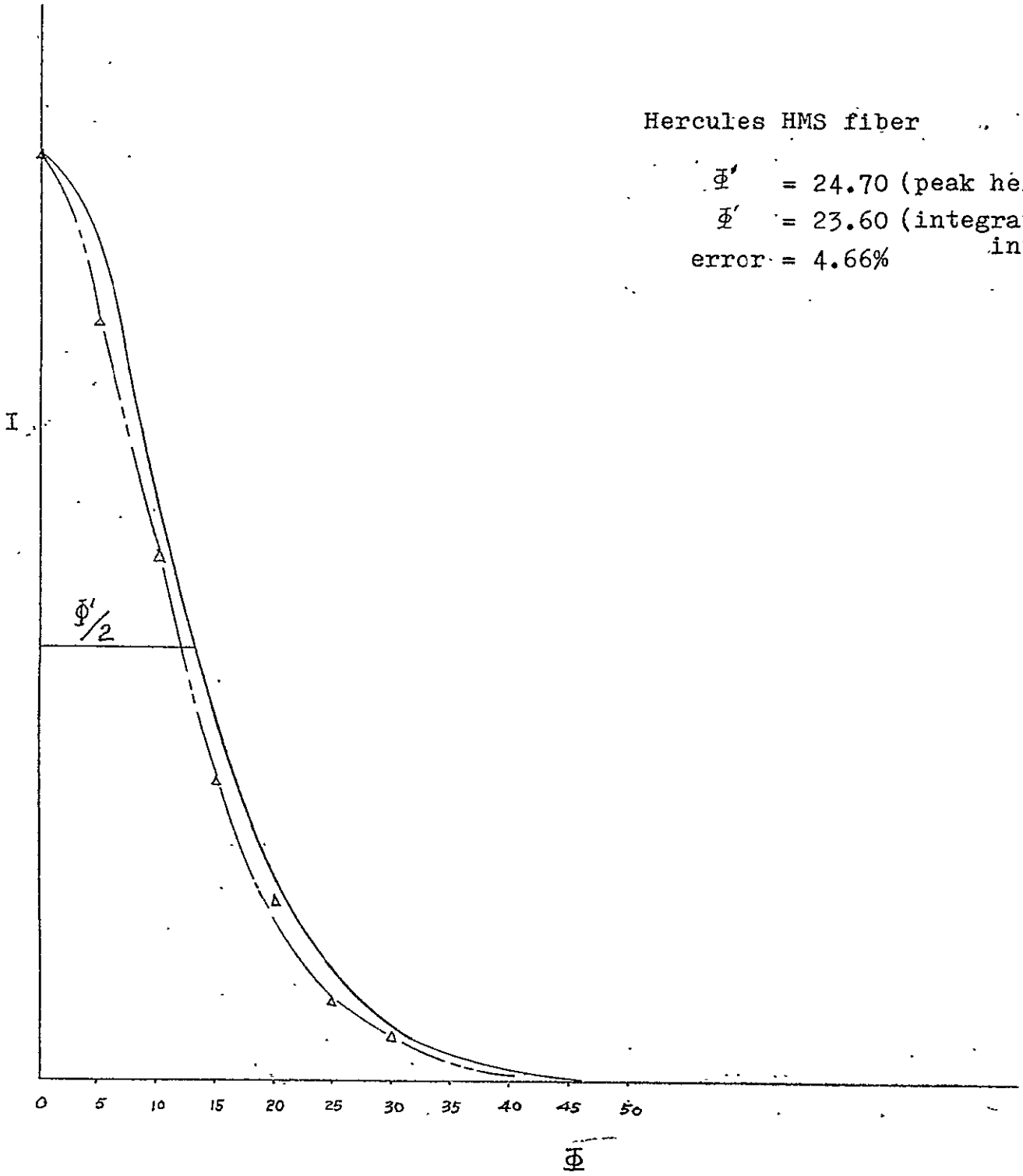
Hercules HMS fiber
Φ' = 24.70 (peak height)
Φ' = 23.60 (integrated intensity)
error = 4.66%
I
Φ'/2
0
5
10
15
20
25
30
35
40
45
50
Φ

FIGURE 26

HERCULES AS FIBER - COMPARISON OF PEAK HEIGHTS vs. INTEGRATED INTENSITY (FROM FIG. 23) FOR PREFERRED ORIENTATION EVALUATION.

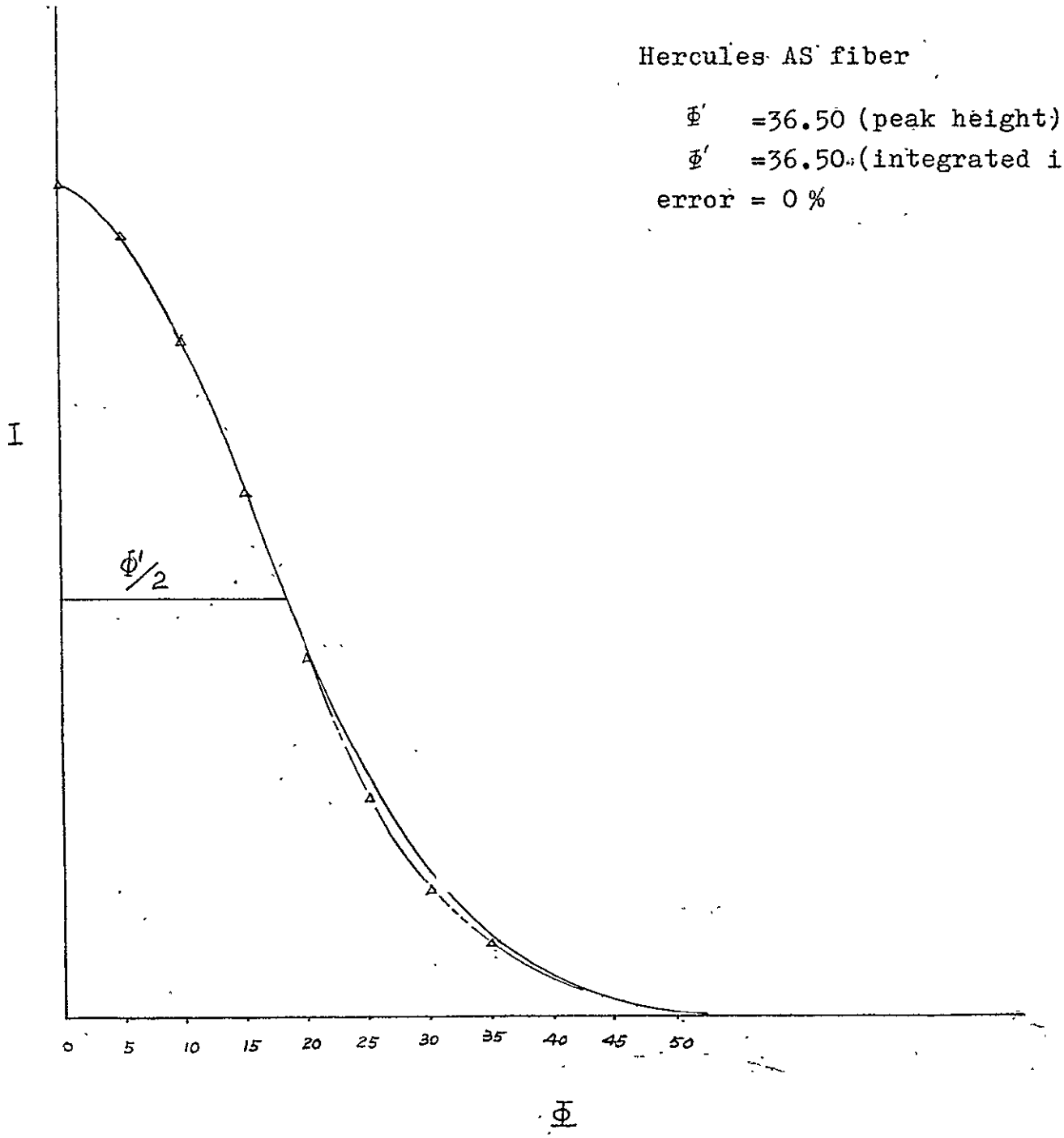
Hercules AS fiber
Φ' =36.50 (peak height)
Φ' =36.50 (integrated intensity)
error = 0 %
I
Φ'/2
0
5
10
15
20
25
30
35
40
45
50
Φ

results indicate that the error in using the peak height method increases with the preferred orientation of the fiber. However, in all cases the error incurred by using the peak height method, even for highly preferred fibers, was less than 10%.

TABLE V

COMPARISON OF PREFERRED ORIENTATION MEASURED BY THE PEAK HEIGHT AND INTEGRATED INTENSITY METHODS

	ϕ' (Peak Height)	ϕ' (Integrated Intensity)	Error
Pitch Fiber	19.05	17.50	8.86%
HMS Fiber	24.70	23.60	4.66%
AS Fiber	36.50	36.50	0%

V. HOMOGENEITY OF RESISTIVITY THROUGH CARBON FIBERS

From the study of preferred orientation of carbon fibers one finds that surface layers of carbon fibers have a structure close to that of pyrolytic graphite with the planes of carbon atoms aligned in the direction of fiber axis. At the interior of a carbon fiber planes of carbon atoms are less well aligned than that at the surface (lower preferred orientation). This inhomogeneity in structure should likewise cause a gradient of resistivity from the surface to the interi but of very much lower magnitude. The increase in resistivity would approximately be equal to the increased pathlength caused by the undulating basal planes. Hence, it was not surprising that the resistivity at the interior of a fiber appears to be the same as that on the surface. The relationship between resistance (R) and the area (A) of a fiber is given by the following equation:

$$R = \frac{\rho \ell}{A} = \rho \ell \left(\frac{1}{A}\right)$$

ρ - resistivity of a carbon fiber

ℓ - length of carbon fiber

If the resistivity does not change within a carbon fiber, then a plot of resistance vs. $\frac{1}{\text{Area}}$ data will result in a linear relationship with the slope of the line equal to ($\rho\ell$ - resistivity times length of carbon fiber). For two Hercules HMS and also AS fibers this linear relationship appears to exist (Fig. 27). We conclude that the change

FIGURE 27

TRANSVERSE ELECTRICAL RESISTANCE GRADIENT
THROUGH CARBON FIBERS.

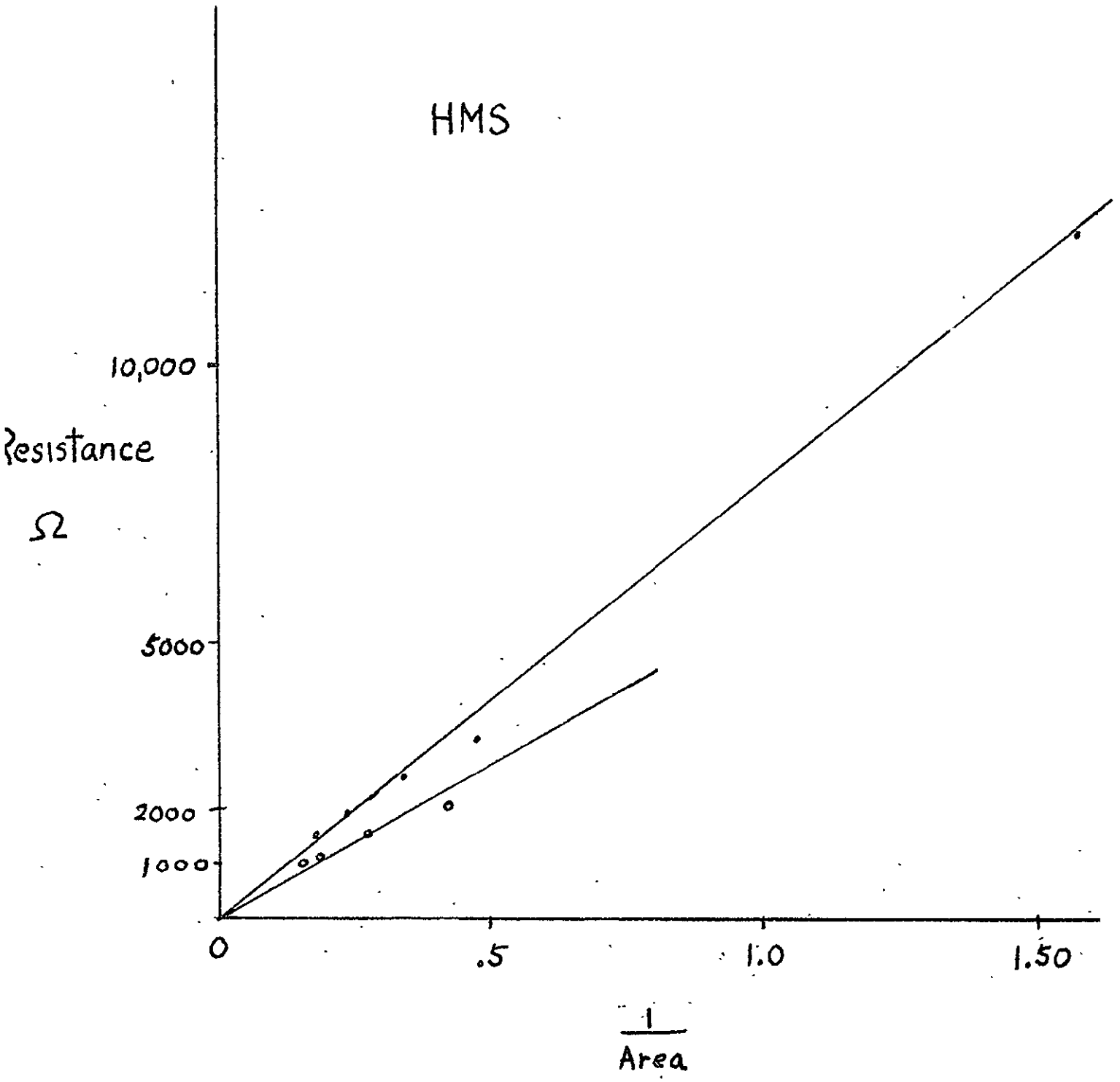
HMS
10,000
Resistance
Ω
5000
2000
1000
0
.5
1.0
1.50
1
Area

in resistivity through a carbon fiber is small compared to the change in modulus. Hence, the preferred orientation should always be maximized to maximize modulus conductivity for a carbon fiber.

VI. DOPING OF CARBON FIBERS

Low temperature-heat treated carbon fi similarly to semiconductors with a small bandgap. This led to attempts to dope carbon fibers with both electron donors (nitrogen) and hole sites (boron). Also some work was performed to make boron/nitrogen/carbon ternaries. Two methods were used to infuse these dopant atoms into carbon fibers: 1) direct diffusion from a gas containing dopants; 2) ion implanation. Attempts to hinder the outward diffusion of nitrogen atoms from stabilized PAN precursors at carbonization temperatures shows no effect. Forceful implantation of nitrogen atoms using ion implantation techniques also showed no effect on electrical resistance of carbon fibers. Preliminary work on diffusion of boron atoms into stabilized fiber showed that this process increased the electrical conductivity of carbonized fibers.

VII. CONCLUSIONS AND FUTURE DIRECTIONS

A thin coating of BN on carbon fibers should eliminate most electrical problems caused by carbon fibers. A coated carbon fiber appears to have lower modulus since

the present low anisotropy BN coating adds little additional stiffness to a fiber.

Future research is directed toward improving the modulus of carbon fibers. The goal is to obtain higher modulus fibers than presently capable at any graphitization temperature. Once the higher modulus fibers are obtained one can then opt to carbonize or graphitize at lower temperatures to obtain higher resistance carbon fibers.

This work on boron nitride coated carbon fibers may have an added benefit in graphite-aluminum composite materials. The surface coating is expected to promote wetting and reduce chemical reaction during fabrication. It would also reduce galvantic corrosion of aluminum in contact with carbon fibers.

APPENDIX A - Resistivity

Resistivity is defined with the followin equation,

$$R = \rho \frac{l}{A} \tag{A1}$$

With Fig. 1 above equation can be changed to the following equation,

$$R = \rho \frac{r}{A} \tag{A2}$$

Or,

$$dR = \rho \frac{dr}{A} \tag{A3}$$

$$= \rho \frac{dr}{2\pi rL} \tag{A4}$$

Therefore,

$$R = \frac{\rho}{2\pi L} \int_{r_i}^{r_o} \frac{dr}{r} = \frac{\rho}{2\pi L} \ell n \, (r_o/r_i) \tag{A5}$$

Therefore,

$$\rho = \frac{2\pi RL}{\ell n \, (D_o/D_i)} . \tag{A6}$$

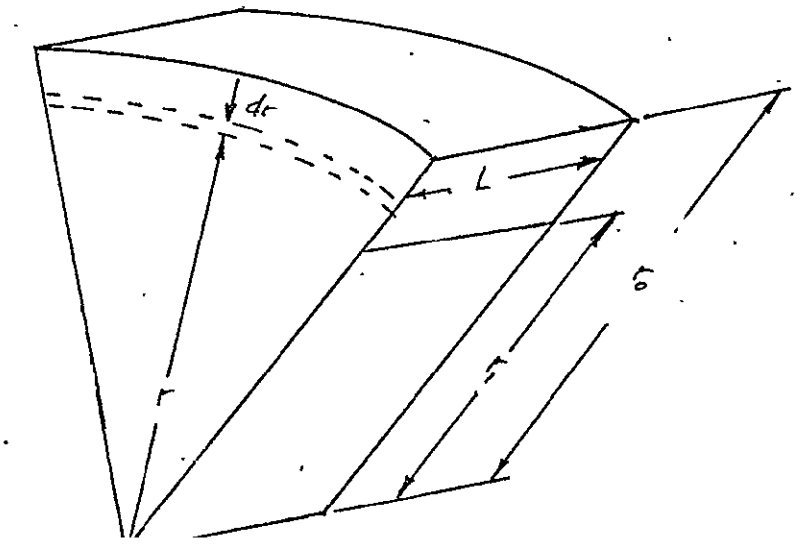

APPENDIX FIGURE 1